3-16-2017

Cytotoxic and antimicrobial effects of silver-containing surfaces

Sarah Goderecci
Rowan University

CYTOTOXIC AND ANTIMICROBIAL EFFECTS OF SILVER-CONTAINING SURFACES

by

Sarah S. Goderecci

A Thesis

Submitted to the
Department of Chemistry & Biochemistry
College of Science and Mathematics
In partial fulfillment of the requirement
For the degree of
Master of Science in Pharmaceutical Sciences
at
Rowan University
July 8, 2016

Thesis Chair: Dr. Gregory A. Caputo

Dedication

To my father,

This manuscript is dedicated to my father, who has provided overwhelming support and encouragement while I continued to pursue my degree, although he seldom understood what I was talking about when he asked what I was doing in school. None of my accomplishments would have been possible without his love and the work ethic he instilled in me; all I've done and all I continue to do is to make him proud.

Acknowledgments

To my family and friends,

I would like to acknowledge my family and friends for their support and understanding of the importance of this research to me throughout this process and with whatever I choose to do going forward. In addition, I would like to thank my research advisor for the time and effort he devoted towards developing me as a scientist and a professional. I would not have thought to pursue this degree without his encouragement, and the skills and knowledge I've gained in pursuit of this degree will no doubt carry forward in my future endeavors.

Abstract

Sarah S. Goderecci
CYTOTOXIC AND ANTIMICROBIAL EFFECTS OF SILVER-CONTAINING SURFACES
2016 - 2017
Gregory A. Caputo, Ph.D.
Master of Science in Pharmaceutical Sciences

This study examines applications of sputtered silver coatings as alternatives to traditional antibiotic treatments. Given the increase in reports of antibiotic-resistant bacteria, new treatments and coatings for in-dwelling medical devices such as catheters and orthopedic implants are necessary. Silver oxide films were deposited onto Ti surfaces to examine the efficacy of such coatings against a variety of bacterial species both *in vitro* and *in vivo*. Bacterial growth studies showed that coatings exhibited antimicrobial activity against a range of bacterial species acting either in a bacteriostatic or bactericidal mechanism, depending on the target. Limited toxicity to *in vitro* mammalian cells was evident in the immediate area proximal to the disc and preliminary studies in a murine infection model show the ability of immunocompetent animals to clear silver from the system. In addition, AgO was examined as an additive to silk biopolymers to add antimicrobial activity for future application in liquid bandages. Silver oxide sputtered films were applied to standard bandages to compare their efficacy to that of commercially available antibiotic-loaded bandages. Silver oxide/copper oxide mixtures were sputtered onto high-density polyethylene to determine efficacy and potentially modulate Ag^{+} release rates. Preliminary results of these studies indicate that AgO-impregnated biopolymers, silver oxide-sputtered silk films, silver bandages and silver oxide/copper oxide mixtures exhibited some efficacy against a variety of bacterial species.

Table of Contents

Abstract v

List of Figures ix

List of Tables xii

Chapter 1: General Introduction 1

- Antibiotic Resistance 1
- Health and Medical Devices 5
- Silver as an Antimicrobial 7
- Silver Toxicity in Humans 9
- Our Study 10
  - Silver-Coated Titanium 11
  - Alternative Modes of Silver Delivery 11

Chapter 2: Antimicrobial Activity of Silver Oxide Containing Thin Films 19

- Introduction 19
- Materials and Methods 22
  - Generation of Silver-Containing Films 22
  - Bacterial Culturing 23
  - ICP-MS Analysis 24
  - Mammalian Cell Toxicity Assays 25
  - Statistical Analysis 25
- Results 26
  - Deposition and Characterization of the AgO Films 26
  - Effects of AgO Coated Discs on Bacterial Growth in Solution 26
  - Silver Ion Release into Culture Media 28
  - Silver Absorption by Bacteria 30
  - Ag_xO Cytotoxicity in Mammalian Cell Culture 31

Table of Contents (Continued)

Discussion....31

Conclusion....38

Chapter 3: Efficacy of Silver Oxide Coatings *In Vivo*....43

Introduction....43

Materials and Methods....45

Bacterial Culturing....45

ICP-MS Analysis....45

In vivo Bacterial Adhesion Assay....46

Results....46

Effect of Silver-Coated Discs on Bacterial Growth....46

Toxicity of Ag_xO Coatings in NIH3T3 Cell Lines....47

Establishing the *in vivo* Bacterial Adhesion Assay....47

Determining the Safety of Ag_xO-Coated Discs *in vivo*....48

Discussion....49

Conclusion....52

Chapter 4: Extension of Silver Oxide Coatings to Materials for Biomedical Applications....58

Introduction....58

Materials and Methods....61

Generation of Silk Films and Silk Film Deposition....61

Rhodamine Release Assay....62

Bacterial Culturing....62

Modified Minimum Inhibitory Concentration (mMIC)....62

Bacterial Growth Curve Analysis....63

ZOI....63

Results....63

Table of Contents (Continued)

Silk Biopolymers as an Antibacterial Delivery Platform 63

Application of Coatings Formed by Reactive Sputtering Applied to Bandages 65

Evaluation of Ag_xO/CuO Films as Next-Generation Antimicrobial Coatings 65

Discussion 66

Conclusion 69

References 81

List of Figures

Figure Page

Figure 1. Resistance to beta-lactam antibiotics 12

Figure 2. SEM image of a mixed phase sample of silver oxide deposited at 20 mTorr in a 67/33 mixture of Ar/O_2 on a titanium foil substrate 32

Figure 3. Antibacterial activity of Ag_xO coatings in liquid culture 33

Figure 4. Zone of inhibition assay 34

Figure 5. Growth curve analysis in media pre-conditioned by exposure to Ag_xO coated (150 nm, double-sided, 1/4") discs 35

Figure 6. ICP-MS analysis of Ag+ released from Ti discs with a single-sided 150 nm thick Ag_xO coating in (A) water, (B) PBS, (C) LB broth, and (D) DMEM for each media type 36

Figure 7. ICP-MS analysis of Ag+ from growth curve samples shown in Figure 3 37

Figure 8. Mammalian *in vitro* toxicity assays 38

Figure 9. Effect of initial culture density on antimicrobial efficacy 39

Figure 10. Effect of increased culture density on antimicrobial efficacy 40

Figure 11. Growth curve analysis using varying numbers of 1/8" Ag_xO test discs for (A) and (B) *E. coli*, and (C) and (D) *S. aureus* 41

Figure 12. Spot platings for both bacterial species at varying time points during the pre- conditioned media assay 42

Figure 13. Effect of initial culture density on antimicrobial efficacy 53

Figure 14. Silver concentration following exposure to various discs and times 54

Figure 15. Detection of luminescent bacteria *in vivo* 55

Figure 16. Blood analysis of mice subcutaneously implanted with Ag_xO-coated discs 56

Figure 17. Ag_xO coated discs do not appear to cause damage to cutaneous tissue.....57

Figure 18. Secondary structure of one *B. mori* silk fibroin chain; (Gly-Ala-Gly-Ala-Gly- Ser) amino acid repeat units that self-assemble into antiparallel beta sheets 71

Figure 19. Rhodamine release comparison form multi-layered silk films 72

Figure 20. Silk films deposited on the bottom of 96 well plate.....73

Figure 21. Modified minimum inhibitory concentrations for *S. aureus*.....74

Figure 22. Zone of inhibition analysis for various silk films containing silver.....75

Figure 23. Growth curve analysis in solution.....76

Figure 24. Zone of inhibition testing for various bandage types.....77

Figure 25. Growth curve analysis of bandages in solution.....78

Figure 26. Zone of inhibition testing for silver oxide/copper mixtures.....79

Figure 27. Growth curve analysis of copper oxide/silver oxide mixtures.....80

List of Tables

Table Page

Table 1. Ag^{+} Elution Rates in Various Types of Media 42

Table 2. Ag_xO/CuO Coating Compositions 80

Chapter 1

General Introduction

Antibiotic Resistance

Since earliest recorded history, civilizations understood the importance of eliminating harmful bacteria and preventing infections, although it was impossible to fully understand the cause of such diseases. It was the discovery of Penicillin in 1928 that led to the "Golden Age" of antibiotic development; multiple new antibiotic drugs were discovered, leading people to believe that all infectious diseases could be cured using antimicrobial drugs[2]. Only ten years following the beginning of penicillin treatment, it was identified that a number of bacteria from the Typhoid-coli group of were not inhibited by the antibiotic, thought to be due to their ability to produce an enzyme[3-4] that was able to degrade the antibiotic. Emergence of antibiotic resistance has followed the development of each new antimicrobial drug since that time, and has become an increasingly devastating and equally challenging obstacle to overcome.

Antimicrobial resistance has proven a worldwide problem, despite differences in application and availability of specific antibiotic drugs in different areas of the world. In the United States alone, the Center for Disease Control estimated that at least 2 million people are infected with antibiotic-resistant bacteria each year, with at least 23,000 dying as a direct result[5]. Although sometimes difficult to quantify the size and scope of resistant infections, one study estimates the cost of treating ear infections alone as having increased 20% between 1997 and 1998, costing approximately $216 million. In this study, infections were caused by only three bacterial species: *S. pneumoniae*, *H. influenzae*, and *M. catarrhalis*[6]; this study provides a small glimpse into the true cost of

antibiotic resistance, yet the larger picture has the potential to be far more devastating. In addition, because of the financial burden associated with resistance development, there has been a lack of new drugs in the development pipeline, which poses an even greater impact for antibiotic resistance. These factors are among the many that are prompting research into alternative antimicrobial approaches, including shifting the focus from antibiotic treatments to infection control and therapies that have reduced likelihood of resistance development in an attempt to combat further diminished effects of current antibiotics.

Understanding the mechanisms by which bacteria overcome an antibiotic is the first step in finding alternative therapies. The ability of many types of bacteria to quickly adapt and evolve is one of the underlying mechanisms used to develop resistance. Antibiotic resistance development can be classified in two broad categories: intrinsic or acquired resistance. In the case of intrinsic resistance, the inherent, molecular, and physiological composition of the bacteria presents barriers to the action of an antibiotic. Most notably, membrane permeability, or the lack of specifically targeted enzymes, is the most common causes of intrinsic resistance. Acquired resistance, however, is much more complex. In this scenario, the bacterium has come into contact with a plasmid that contains determinants for resistance, or the bacterium previously underwent a chromosomal mutation, which would allow it to be resistant to the antibiotic. At this point, the mechanisms for resistance become dependent on the plasmid acquired or the mutation[2]. One such example of plasmid-mediated antibiotic resistance is quinolone resistance, which was thought to originate from a genetic mutation, yet the discovery a multi-resistant plasmid with the ability to encode for quinolone resistance has changed

the general understanding of the underlying mechanism of this type of resistance[7]. The downstream effects of these genetic alterations result in either enzyme production to degrade the drug, modification of the drug target, and/or enhanced active export of the drug[2].

When prescribed an antibiotic for an illness, patients are instructed to take the correct dosage each day for a set number of days to ensure that the source of the infection is completely eradicated. In some cases, whether due to antibiotic misuse, overuse, or due to bacterial survival mechanisms, viable bacteria remain in the patient even after treatment. More recent studies have suggested that bacteria can also overcome antibiotics collectively[8], rather than only some individuals surviving to replicate and produce an infection requiring stronger antibiotic treatment. Regardless of the amount of bacteria that become tolerant to treatment, antibiotic tolerance is a definite precursor to resistance, and should be taken into account by prescribers and patients alike.

Overprescribing antibiotics has become a major cause of resistance development, especially in wealthier nations where antibiotics are more easily available. Worldwide antibiotic consumption is a rising trend, and the over-the-counter availability in some nations has increased usage in those areas, even despite the medication's high cost[9]. In China, some hospitals are offered an incentive for antibiotic sales, which drives overprescribing; one study estimated that ¼ of the total revenue for two hospitals was exclusively due to the sale of antibiotics[10]. The World Health Organization published a study in 2014 analyzing bacterial resistance in 129 nations with a variety of average income levels. The data shows that a majority of the resistant cases of *E. coli*, *K. pneumoniae*, and *S. aureus* originated in upper-middle income or high-income nations,

but no reports were available for low income or low-middle income countries. This report, although helpful, highlights another inconsistency in the available data: there is no protocol in reporting antibiotic-resistant cases globally, and therefore no comprehensive data on the scope of resistance across the globe[1]. In addition, the World Health Organization estimates that the size and scope of antibiotic resistance to classes such as beta-lactams (Figure 1) is affecting the population on a worldwide scale.

The use of antibiotics in agriculture and food production is another major factor in the growth and spread of resistance. Extensive research has been done as to the mechanism of growth benefit when administering sub-therapeutic levels of antibiotics to food-producing animals. Hypotheses of these studies include the inhibition of harmful bacteria which may be mildly pathogenic, inhibition of bacterial urease, improved efficiency of the gut, nutrient sparing, improved nutrient absorption from morphological changes to small intestinal epithelium, and reduced immune stimulation[11]. One study shows an estimated 70% of antibiotics used in the United States are consumed by animals, as compared to the 50% used for agricultural purposes internationally[12]. As explained previously, agricultural antibiotic administration poses the risk of enteric bacteria in these animals developing tolerance to the administered drugs. This introduces the prospect of antibiotic resistance developing across multiple species, and in 2014 there were multiple gene discoveries in food-producing species that code for antibiotic resistance[13]. Regardless of the benefits of antibiotic administration in agricultural settings, it has been confirmed by one extensive study that the use of antibiotics in food-producing animals can translate antimicrobial resistance profiles to humans that consume them[14]. In many cases, antibiotic-resistant genes have been found in both packaged meat

and human isolates[15]; bacteria, after ingestion by consumption or preparation, have been found to survive in the human body for up to fourteen days[16], enough time to induce infection in its host.

Health and Medical Devices

In 2011, the CDC estimated that 721,800 hospital infections occurred in the United States, accounting for 1 in every 25 hospitalized patients that year[17]. Of these infections, pneumonia and surgical site infections occurred in the highest number of cases (22%), followed by gastrointestinal infections (17%), urinary tract infections (13%), and bloodstream infections (11%). In these cases, some of the most common causes of these infections were *C. difficile* (12%), methicillin-resistant *S. aureus* (MRSA) (11%) and *E. coli* (9%). Although recent reports show that hospital-acquired infection rates are on the decline[18], alternatives to traditional cleaning procedures and treatments are becoming widely investigated.

Preventing infections has become a goal of both the scientific and medical communities in an attempt to reduce antibiotic usage and stop the spread of resistance. This practice is becoming increasingly common in the realm of orthopedic surgeries, due to the difficulty of treatment and clearance of osteomylytic infection (interior of the bone). Stronger antibiotic courses as well as implant retrieval/replacement are common in implant-related osteomyelitis. As such, surgical intervention related to infection control yields negative outcomes such as patient stress and prolonged hospital stay, all of which can cost upwards of $50,000 per instance[19].

Infections in orthopedic surgeries have become increasingly more prevalent due to the ability of bacteria to adhere to the surface of the implant[20], although the body's natural immune defenses are boosted following surgical stresses. Should enough bacterial cells adhere to the surface of the implant in close special arrangement, biofilms can be created on the surface of the implant[21]. Briefly, biofilms, whether made up of a single bacterial division or multiple species, have proven far more resistant to standard antibiotic treatments, and in most cases, removal and replacement of the implant is the only viable option for complete recovery. The mechanism in which biofilms resist antibiotic activity is somewhat variable between species, yet in the case of *P. aeruginosa*, for example, it was found that periplasmic glucans synthesized by the bacteria have the ability to interact directly with administered antibiotics, which prevents them from reaching their site of action[22]. This mechanism of resistance is only one example of how biofilms can resist antimicrobials, making them anywhere from 10-1,000 times more difficult to irradiate than the planktonic bacteria[23]. In the United States alone, the total yearly cost for treatment of biofilm infections is estimated to be $94 billion, while infections are responsible for half a million deaths[24].

There are multiple proposed methods for preventing infections post-surgery, including preventing bacterial adhesion and absorption, various methods to kill bacteria, and 'smart coatings' for implants[25]. Of these, the practice of applying a surface coating to the implant has become the most popular, due to lack of continued maintenance and near-identical surgical procedure as that of a non-coated implant[26]. Coating orthopedic implants could potentially inhibit bacteria from adhering to the surface of the implant, therefore preventing or reducing biofilm growth and therefore, subsequent infection.

Silver as an Antimicrobial

Silver was first documented as having been used by early civilizations as a water purification tool; silver coins and silver vessels were used to hold and purify collected water[27]. The first documented medical use of silver occurred between 705-750 CE, although it was most likely used prior to that time for medicinal purposes. Despite the lack of knowledge by early civilizations about microbial infections, it became overwhelmingly evident that silver therapies were viable cures for various conditions. In the following years, silver was used as treatments for eye infections, surgical dressings, burn wounds, ulcer treatments, and compound fractures[28-29]. The first silver-resistant bacteria were identified in the 1960s from a burn wound treated with silver nitrate[30], and have since been identified in both clinical settings as well as environments where silver is naturally-occurring[31-32]. The resistance mechanism, although not completely understood, is thought to be similar to resistance mechanisms of bacteria against others metals (Cu, Zn, etc.)[32], and although published evidence is scarce, has only been associated with high quantities of silver over frequent time periods[33].

Silver's antimicrobial properties arise from the presence of the silver ion (Ag^+)[33], although the exact mechanism of action is still unknown. Many proposed theories on the mechanism of action of Ag^+ deal with interactions at the bacterial cell membrane, which can affect membrane permeability, cause inhibition of both the proton motive force and respiratory transport chain, all of which result in cell death[27, 33-34]. Based on suspected mechanisms, silver can be considered a viable candidate for broad-spectrum antimicrobial activity, despite not knowing the frequency or identity of its targets.

There are multiple delivery methods and product forms of silver on today's market, yet the common element between each is the delivery of silver ions to the affected area. Selected product forms are also dependent on the context in which silver is being administered, the solubility profile of the environment, and longevity of activity. Currently, silver nanoparticles are considered an efficient method of delivery, largely due to their customization profiles and variability. In addition, colloidal silver has been a popular 'cure-all' remedy, and can be purchased in any number of places. Silver inorganic complexes, such as silver sulfadiazine, silver nitrate, silver chloride, and silver oxide are also particularly favorable[35] but can be difficult to administer due to low solubility in water.

Silver Toxicity in Humans

Although silver is found in many aspects of the environment, it is not considered naturally occurring in the human body, nor is it acknowledged as a trace element. Absorption through food and drink can provide detectable low levels of silver in the bloodstream[36], these levels have not proven to impact normal function, nor cause excessive buildup in organ tissues[37]. In cases of prolonged silver exposure or extended treatment, the most widely-reported side effect is a blue-gray discoloration of the skin or soft tissue, referred to as argyria[38]. In cases such as these, silver accumulation was reported in such tissues as the skin, kidneys, liver, corneas, mucous membranes, nails, and spleen[37, 39-40] although in the majority of cases, silver deposition was merely cosmetic, and is not known to be life-threatening[41].

There is some concern regarding the possible neurotoxicity of silver, as well as the ability of silver ions to cross the blood-brain barriers and induce negative neurologic effects[42-43]. There are at least nine known metals that have been found to accumulate at the blood-brain barrier and gain access to neurologic tissues, including the toxic metals lead, cadmium, and mercury[41-42]. Silver-induced neurotoxicity is believed to be rare[43], however one clinical study showed the effect of colloidal silver as a nasal spray for 2-5 years on an elderly patient. In a necropsy examination of the brain, significant silver deposits were found in only part of the choroid plexus portion, while the majority of brain parenchyma tissue appeared normal[43-44]. Further investigation of the possible neurotoxicity of silver are needed before definitive determinations can be made regarding the safety of silver therapy over extended periods of time.

Our Study

Adding a coating to the surface of titanium implants has become an increasingly popular tactic in dealing with infection caused from surgery[45]. Previous work has shown that using a sputtering technique, silver can be applied in thin coatings to titanium surfaces with good adherence, and such coatings were shown to prevent bacterial adhesion to the surface[46]. The goal of this work was to develop and characterize coatings that can adhere to surfaces appropriate for medical devices, elute some or all of the material from the coating as an antimicrobial in solution, and develop an understanding of the release dynamics of the eluted materials. Using a modified reactive-sputtering approach, we have applied silver oxide coatings that retain the same materials properties as pure silver coatings, but can also elute Ag^{+} from the surface, which act as an antimicrobial in solution. Coatings that elute from a surface are useful in healthcare

applications due to their ability to not only prevent adhesion of bacteria to the surface, but to kill any bacteria in the immediate area, allowing for maximal wound healing with minimal or no antibiotic intervention. This coating approach is potentially useful for titanium orthopedic implants as well as catheters, medical instruments, hospital surfaces, and other objects at high-risk for bacterial contamination and/or infection.

Silver-coated titanium. Silver-sputtered titanium discs, used to simulate orthopedic implants, were subsequently tested for antibacterial activity in solution. Coatings containing different thickness and chemical composition were tested against a variety of bacterial species to assess broad-spectrum antimicrobial efficacy, as supported by previous results from our lab and the literature. In addition, release rates of silver from the coated discs in various media types were studied to determine any relationship between rate of release and antimicrobial activity. Furthermore, efficacy and toxicity studies are ongoing to assess how sputtered coatings react in *in vitro* and *in vivo* systems using mammalian cell culture models, as well as a murine infection model.

Alternative modes of silver delivery. Silk is a biocompatible protein polymer, derived from biological sources which degrades into non-toxic products *in vivo*[47], making it ideal for biomaterial delivery systems. Silk solutions formulated from *Bombyx mori* caterpillar cocoons were treated and formulated to include various percentages of silver oxide, or coated with silver oxide deposited via reactive sputtering. To assess the antimicrobial properties of the impregnated and coated silk material, films were deposited on the bottom of 96 well plates for analysis. Release rates and antimicrobial properties for these films were assessed in solution against various bacterial species. To extend the scope of applications for these coatings, silver-coated bandages were also investigated,

and were compared against standard bandages and commercially available antibiotic-loaded bandages. Current and ongoing experiments are focusing on the antimicrobial properties of copper and copper oxide/silver oxide mixtures. Copper oxide's poor solubility profile proved to affect its antimicrobial efficiency, whereas the silver oxide/copper oxide mixtures were the most effective in killing bacteria.

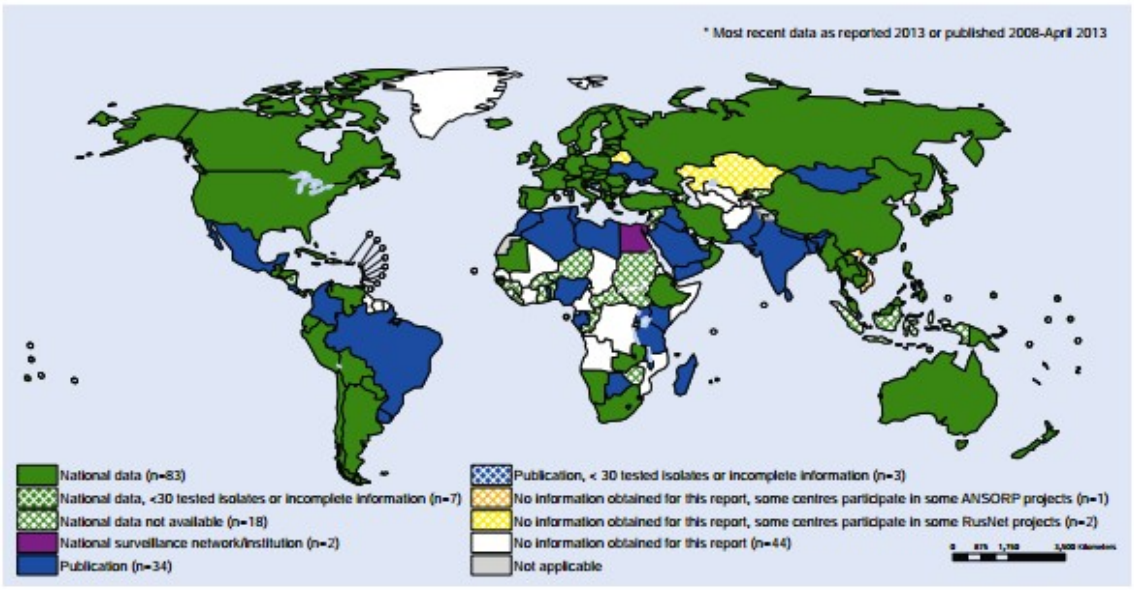

Figure 1. Resistance to beta-lactam antibiotics [1].

Chapter 2

Antimicrobial Activity of Silver Oxide Containing Thin Films

Introduction

Antimicrobial resistance has proven to be an obstacle of overwhelming importance to both the medical and scientific communities following the introduction of antibiotics in the early 20th century[2]. The ability of many bacteria to adapt to changing environmental conditions can be at least partly a result of their ability to overcome pharmaceutical approaches intended to eradicate them. Routine and improper antibiotic use is partially responsible for the selective pressure that ultimately provides advantages for mutant bacterial strains; those strains have proven far more costly to treat, and often require longer hospital stays in comparison to strains that are susceptible to traditional, small-molecule antibiotic treatments[4]. In addition, intrinsic resistance is another factor in the resistance cascade: the low membrane permeability of certain bacterial strains makes antibiotic penetration of the membrane nearly impossible[2].

Preventing infections is a goal of both the scientific and medical communities in an attempt to reduce antibiotic usage and stop the spread of resistance. Infection control has become a significant concern in many areas of medicine but is especially critical in orthopedic surgery due to the invasive measures that must be taken when infections develop post-surgery which are extremely difficult to treat with antibiotics alone. The restricted access around surgical implants results in the need for stronger and longer antibiotic courses and increased potential for implant retrieval, debridement and device replacement. Additional surgeries result in increases in patient stress and prolonged hospital stay[19]. Some studies estimate that 2.5% of primary hip and knee arthroplasties

and up to 20% of revision arthroplasties develop a periprosthetic joint infection, with the mortality rate for these infections nearly 2.5%[9]. Current research estimates that if there are no successful efforts to combat the spread of resistance, the number of annual deaths could increase from the current 700,000 to as many as 10 million by the year 2050[48].

Silver has been used for thousands of years in different civilizations for numerous applications including food and water purification, ulcer treatments, promoting wound healing, as well as prevention of surgical infections[29]. Antimicrobial studies using silver compounds show its efficacy against a wide range of bacterial species including *B. subtilis*, *E. coli*, *P. aeruginosa, P. vulgaris*, and *S. aureus*[49-52]. The exact antimicrobial mechanism of silver is not fully elucidated, but the ability of silver to act against multiple bacterial species suggests that silver interacts with multiple bacterial target sites, most readily with the thiol groups of cysteine residues[53]. This is consistent with the high abundance of thiol groups in bacterial cell membranes, and silver exhibiting a broad-spectrum antimicrobial activity profile. At the bacterial cell membrane, ionic silver inhibits the proton motive force (PMF), the respiratory electron transport chain, and affects membrane permeability, all of which can result in cell death[27, 33-34]. Although different forms of silver are available, the ones most readily available fall into three categories: elemental silver, inorganic silver complexes, and organic silver complexes[33].

Many varieties of silver materials are used in both healthcare and medical device industry, yet the release of silver ions from the complex is what ultimately determines the compound's antimicrobial efficacy[54]. The primary drawback of pure silver is the poor aqueous solubility, which limits the ability to act as an antimicrobial over meaningful distances from metallic surfaces. Considering the silver ion Ag^{+} is the likely

antimicrobial form, efficient solubilization in the environment is necessary for activity beyond the surface[46]. There are a variety of silver-containing complexes that enhance the solubility of silver[54]. Silver oxide has low solubility in water, however it generates enough soluble silver ions to effect antimicrobial activity in several applications[55-56]. Our previous work has shown that silver oxide can be efficiently deposited as thin-film coatings on a variety of surfaces and retains the ability to generate sufficient concentrations of Ag^+ to exert antimicrobial activity[57].

Thin film coatings of silver oxide can be applied to orthopedic implants in an effort to inhibit bacteria from attaching to the surface of the implant, therefore preventing/reducing biofilm growth and subsequent infection. The solubility of silver oxide also allows for antimicrobial activity distal to the implant surface, which can ameliorate infections in the area of the implant. To further examine the antimicrobial efficacy of the silver oxide thin film coatings, parameters such as coating thickness, rate of release of silver ions from the surface, and initial cytotoxicity to in vitro mammalian cell systems were investigated. The work reported here indicates that relatively short exposure of silver oxide thin films to a culture was sufficient to inhibit bacterial growth. Additionally, the release of Ag^+ ions from the films was not significantly impacted by the culture medium, but efficacy and toxicity were related to total silver concentration in solution.

Materials and Methods

Generation of silver-containing films. Thin films of cubic silver oxide (AgO) were grown reactively in a custom designed two-cathode sputter deposition chamber.

Each of the cathodes contains a two-inch diameter silver target with 99.95% purity. The cathodes are in a confocal configuration pointing upward toward a sample holder that is 2.54 cm x 5.08 cm. The gas mixture used is 67% argon and 33% oxygen adjusted using two mass flow controllers. Argon is adjusted to a rate of 20 sccm while oxygen flows at a rate of 10sccm, though other mixtures of argon and oxygen also will work to synthesize bactericidal silver oxide. The pressure in the chamber during deposition is held at 20mTorr controlled by a butterfly baffle valve connected to a capacitance manometer. The chamber is configured with a 360l/s turbopump and backed with a Drytel 1025 vacuum pump. The working distance, the distance from the silver target to the substrate, is approximately 8.89 cm.

Each of the cathodes is powered using a MDX-500 DC-power supply applying a power of 25 W to each cathode. In the chamber configuration, the deposition rate is approximately 17 nm/min. X-ray diffraction results indicate that the coatings are a combination of cubic phases of AgO and Ag_2O (henceforth referred to as Ag_xO)[57]. The microstructure of the coatings is measured using a field emission scanning electron microscope (JEOL 7500).

Bacterial culturing. Bacteria were streaked onto LB - miller agar (Difco) plates from strains stored in a frozen library (*E. coli* MG1655, *S. aureus* ATCC® 25923, *P. aeruginosa* ATCC10145, *K. pneumoniae* 700603). All streaks were stored in a refrigerator at 4°C. To prepare overnight cultures, a single colony of each bacterial strain was added to LB broth (Difco) in sterile culture tubes. Tubes were placed in the shaking incubator at 37°C overnight to allow for sufficient bacterial growth. Following the incubation period, dilutions of the overnight culture were made in Muller-Hinton broth

(Criterion) 1:100; changing broth provides for better short-term bacterial growth and facilitates comparisons to MIC assay protocols.

Bacterial growth analysis. Dilutions were grown to OD_{600} 0.2 - 0.3 before being diluted a second time to the indicated experimental range. Calculations were performed under the assumption that $OD_{600} = 1.0$ is equivalent to $\sim 10^8$ CFU/mL for *S. aureus* and *K. pneumoniae* and $\sim 10^9$ CFU/mL for *E. coli* and *P. aeruginosa*[58-60]. The bacteria were added to fresh Muller-Hinton broth in sterile tubes containing the test piece; total volume in each tube was 3 mL. All experiments with silver-coated discs were performed in at least duplicate for each bacterial species tested. OD_{600} measurements were recorded on each of the cultures every 30 min using ultraviolet-visible spectroscopy; between time intervals, tubes were agitated at 220 RPM in a shaking incubator at 37°C.

Growth in cultures pre-incubated with silver. To prepare silver-soaked broth solutions, MH broth was added to each of the sterile culture tubes, and tubes were placed in the shaking incubator at 37°C. Ag_xO-coated titanium discs were added to each of the tubes at varying time intervals to allow for dissolution of the coating into the solution. Following the selected time periods, the pre-incubated silver-containing broth was transferred to new, sterile tubes. Following the growth of the bacterial dilutions to OD_{600} 0.1 - 0.2, 30 µL bacterial solution was added to each of the pre-incubated broth tubes and the experiment carried out as described. At three different equally spaced time intervals during the kinetics assay, 3 µL was taken from each test tube and plated on LB agar in various positions to assess bacterial growth at those times. Plates were incubated overnight at 37°C.

Zone of inhibition (ZOI) assay. Dilutions were grown to OD_{600} 0.1 - 0.2. Subsequently, 100 µL of bacteria was plated onto lysogeny agar plates and spread using sterile glass beads. Each of the 0.635 cm test discs were placed onto the plate using sterile technique, coated side down, and plates were placed in the incubator overnight at 37°C. Following incubation, plates were moved from the incubator, photographed, and the resulting zones were measured.

ICP-MS analysis. All samples were prepared with deionized water, phosphate buffered saline (PBS, 50mM sodium phosphate, 150mM NaCl, pH 7), sterile LB broth, or DMEM medium. Medium (10 mL) was added to a sample tube, and test discs were subsequently added to the bottom of each tube. Sample tubes were placed in the shaking incubator at 37°C for ten-minute intervals. Following the incubation period, the media was removed and an equal volume of fresh media was added to the sample tube; release experiments were carried out over a one-hour period.

In the case of kinetics sample preparation, cells from 1 mL of culture from each of the tubes used in the growth curve experiment were pelleted for 10 minutes at 6,000 RPM in a Benchmark mini centrifuge. The supernatant from each of these tubes was placed into a new sample tube, and was combined with 5% nitric acid. The pellet containing the bacterial cells was discarded. All ICP samples were run against a standard prepared in 5% HNO_3 containing 1,000 ppm silver nitrate (Ricca) calibrated to fit a linear curve model and contain expected experimental outcome values.

Mammalian cell toxicity assays. NIH3T3 cells (American Type Tissue Culture, Manassas, VA) were cultured in DMEM with 4.5 g/L glucose, L-glutamine, and sodium

pyruvate (10-013-CV; Corning, Manassas, VA) with 10% FBS (35-010-CV; Corning) and 1% penicillin-streptomycin (P0781; Sigma-Aldrich, St. Louis, MO). NIH3T3 ($1.5x10^6$ cells) were plated in a six-well plate approximately 12 hours before adding discs and incubated at 37°C with 5% CO_2. Titanium only (control) or silver-coated titanium discs were gently placed into the wells at the indicated time points before collection. Media was removed and centrifuged to pellet any non-adherent cells; adherent cells were gently trypsinized and pooled with the non-adherent cells for each sample. Cells were collected and stained using an Annexin-V/PI kit (630109; Clontech, Mountain View, CA) and FACs analysis was performed to determine the percentage of apoptotic cells.

Statistical analysis. Student's t-test was performed to determine statistical significance for the mammalian cell in vitro toxicity assays. All t-tests were performed as a comparison to the value for apoptotic cells in the titanium control after 72 hours of incubation. A p-value < 0.05 was considered statistically significant.

Results

Deposition and characterization of AgO films. The result of the microstructural imaging of a 500 nm thick sample on a titanium foil substrate is shown in Figure 2. In the 50 kx image, the lighter regions contain voids at the grain boundaries probably associated with the underlying defects in the cold-worked titanium foils used for substrate materials. Lower oxygen concentrations during deposition yield larger grains and better-defined grain boundaries than the image shown. However, we have no direct evidence that the variations in microstructure impacts the performance of these materials.

Effect of Ag_xO coated discs on bacterial growth in solution. Based on the previous findings of Ag_xO coatings exhibiting antimicrobial activity in solution, measurements were extended to a more detailed analysis of coating properties on efficacy. Figure 3 shows the growth curves of various bacterial species (*E. coli, S. aureus, P. aeruginosa, and K. pneumoniae*) in the presence of an uncoated Ti disc or a Ti disc coated on both sides with ~ 150 nm thick Ag_xO film. In each case, the culture containing the titanium disc exhibited growth comparable to the control culture. In contrast, the cultures containing the Ag_xO-coated discs showed significantly lower OD_{600} values for all bacteria tested. These curves indicate that the Ag_xO coating is eluting from the surface of the disc into solution, inhibiting bacterial growth in all bacterial species. Additionally, this inhibition was almost immediate upon addition of the Ag_xO coated disc to the bacterial culture, indicating the rate of release high enough to very quickly reach a threshold concentration of Ag^+ in the culture to inhibit growth. These experiments were extended to include bacterial cultures with different initial bacterial cell densities and the results were similar (Figure 9).

The design of the experiments in Figures 3 and 9 involve the addition of the Ag_xO coated disc to a bacterial culture in very early log-phase growth ($OD_{600} \leq 0.1$). However, it was of interest to examine how these eluting coatings would behave in actively growing mid-log cultures. As such, Ag_xO coated discs or Ti controls were added to cultures of *S. aureus* or *E. coli* well into log-phase (Figure 10). The results show that the addition of the disc at time 0 caused rapid inhibition of the planktonic culture. The cessation of bacterial growth indicated by a plateau in the OD_{600} was generally seen between 30 - 60 minutes after the addition of the disc. Additionally, aliquots of the

culture at the final time point (t = 3 h) exhibited growth on LB plates, indicating that the Ag^+ released into the culture was sufficient to exhibit bacteriostatic activity but not bactericidal activity (data not shown).

The ability of the Ag^+ to elute from the coatings and inhibit bacterial growth in solution is a promising step toward the development of coatings for device applications. Next, the properties of these coatings to prevent bacterial growth on surfaces, was investigated using a modified Kirby-Bauer zone of inhibition (ZOI) approach. Briefly, Ti discs or discs coated with Ag or Ag_xO films were placed on agar plates seeded with known amounts of bacteria. These plates were incubated and the ZOI was measured following 18 hours of growth (Figure 4). The presence of a ZOI indicates that the Ag^+ ions from the coating eluted and inhibited bacterial growth with this zone. The Ti control disc and the Ag-coated discs both exhibited no measurable ZOI, indicating that the pure silver coatings were unable to elute and diffuse through the solid agar medium to any significant concentration able to prevent bacterial growth. For this reason, as well as the cost of material, pure Ag^+ coatings were used minimally in liquid culture assays (data not shown). In contrast, the Ag_xO coated discs clearly caused a ZOI, ranging from 0.8 - 1.0 cm in diameter. This inhibition of bacterial growth around the disc clearly indicates that Ag^+ is eluting from the disc at high enough concentrations to inhibit bacterial growth.

Silver ion release into culture media. The results above and from previous work[46, 57] support the hypothesis that the antimicrobial activity of the Ag_xO coatings is directly tied to the elution of Ag^+ from the films. This was further examined by pre-conditioning fresh culture media by incubating an Ag_xO coated disk in media for a fixed amount of time before adding a bacterial inoculum. Figures 5A and B show the growth

curves of *E. coli* and *S. aureus* in media that was incubated with Ag_xO-coated discs for variable times. In both cases, media that was pre-incubated for the longest times (30, 60, 120, 240 minutes) prevented the growth of the inoculated bacteria. In the case of *S. aureus*, the 6-minute pre-incubation did not elute enough silver into the media to completely inhibit bacterial growth. However, it is notable that the growth profile of *S. aureus* was significantly inhibited, lagging well behind the growth profile of the untreated control culture. These results indicate that the release rate of Ag^+ from the Ag_xO films is sufficiently fast to reach a threshold concentration in solution to inhibit bacterial growth.

The bacterial cultures grown in pre-conditioned media were investigated to determine if the Ag^+ acted in a bactericidal (killing bacteria) or bacteriostatic (inhibiting bacterial growth) mechanism. At selected time points during the course of the growth curves, a small aliquot of the culture was removed and spotted onto LB-agar plates, which were incubated for 18 hours to allow bacterial growth (Figure 5C). If the Ag^+ is acting as a bacteriostatic agent, the bacteria should become viable upon removal from the Ag-containing culture and grow on the solid media while a bactericidal action would leave no viable bacteria to grow on the plate. Strikingly, the preconditioned media exhibited different mechanisms for the Gram-negative *E. coli* (Spots 1-6 in Figure 5C, taken at 3h time point in the growth curve) compared to the Gram-positive *S. aureus* (spots 7-12, Figure 5C taken at 3h time point in the growth curve). The concentrations of Ag^+ in solution were bactericidal for *E. coli* but were bacteriostatic for *S. aureus*. Aliquots from the cultures were also plated corresponding to different time points (0 and 6h) in the growth curve and similar results were found (Figure 12).

The release of Ag^+ into the pre-conditioned growth media solution was further characterized by inductively coupled plasma mass spectrometry (ICP-MS). ICP-MS is capable of detecting metals and certain non-metals in very low solution concentrations (<0.1 ppm). The results of ICP-MS on LB media that was pre-conditioned for the same time intervals are shown in Figure 5D. These results clearly show an increasing Ag^+ concentration as a function of time, indicating continual release. The longest time point (240 min) exhibits a similar concentration as the previous (120 min) indicating this may be near the saturation point for this media type.

The effect of release rate was also examined by modifying the size of the coated disc used in the experiment. The release rate of Ag^+ will be directly dependent on the surface area of the disc, that is, the surface area exposed to the media and nucleation sites for release. This was performed by exchanging 0.3175 cm diameter discs for the 0.635 cm diameter used in previous experiments, while keeping the composition of the coating the same. Figure 11 shows by decreasing the surface area, a 0.3175 cm disc did not prevent bacterial growth, however by adding two or more 0.3175 cm discs to the same culture, the bacterial growth inhibition was restored.

The concentration of Ag^+ in the pre-conditioned media indicated a time-dependent release profile, consistent with our previous findings. This was extended to examine the effect of environment on the release rates, as the majority of previous reports focused on the release profile in water, while *in vitro* cellular experiments take place in much more complex media. Figure 6 demonstrates the cumulative silver release in water and various media types as measured by ICP-MS. The results show that the Ag^+ elutes at a faster rate in water compared to the more complex media tested (LB used for bacterial

growth experiments and DMEM used for mammalian cell growth conditions). Interestingly, the release rate of simple phosphate buffered saline (PBS) is slower than water but faster than the complex growth media. The overall trend of release rates is H_2O > PBS > LB ≈ DMEM. The release rates calculated from these experiments and statistics are included in the supplement (Table 1).

Silver absorption by bacteria. The results in the previous experiments show that the eluted silver ions are the driving force behind the antimicrobial activity. This was extended to investigate the association of eluted Ag^+ to bacteria in solution. Starting with cultures used in the growth curve experiments in Figure 3, a portion of the culture was pelleted, dissolved in 5% nitric acid, and subjected to ICP-MS analysis. In all cases, bacteria exposed to Ag_xO coated discs displayed significantly higher silver content in the pelleted cells compared to titanium controls (Figure 7). This indicates the Ag^+ ions are stably associated with or are being taken up by the bacteria. It should be noted that the cell pellets for the AgO treated samples were very small compared to the control, as the number of viable cells was much smaller. Additionally, while there was some variability between samples, all bacteria tested exhibited approximately the same amount of Ag associated.

Ag_xO cytotoxicity in mammalian cell culture. Ag^+ ions have been shown to be toxic to mammalian cells at certain concentrations[61]. Therefore, it was of interest to determine whether Ag_xO discs and the eluted Ag^+ from these discs are toxic to murine fibroblasts (NIH3T3 cells) *in vitro*. Cells (1.5×10^5) were seeded in 6-well plates in complete media. Cells were incubated with either no disc, uncoated Ti disc, or Ag_xO coated Ti discs for the indicated times, and apoptosis was analyzed using the Annexin-V

assay. Figure 8 shows that apoptosis significantly increased by 48 hours in cells incubated with discs coated with 150 nm films on one or both sides of the disc. Interestingly, the percentage of apoptotic cells appears to plateau at approximately 40% in both cases. Of note, it was observed microscopically that cells immediately surrounding the disc showed signs of cell stress prior to cells located distally to the disc, which is likely due to an increased local concentration of Ag^+ ions after or during elution (data not shown). Collectively, these data suggest that high silver concentration in the local environment eventually becomes toxic to the local cells.

Discussion

Overall, the experimental results presented show a distinct and rapid inhibition of bacterial cell growth in planktonic culture and on surfaces due to the presence of Ag_xO coatings. This inhibition is clearly linked to the ability of coatings to elute silver ions into solution, or the local environment. The concentration of Ag^+ eluted into solution was directly dependent on the size of the eluting surface, exposure time, and the composition of the coating[46, 57].

As mentioned previously, silver has been used as a method for sterilization for thousands of years[62]. Notably, in that time, there has been limited development of resistance to silver[33]. The lack of resistance development is credited to the ability of silver to induce response in a variety of targets in bacterial cells, both membrane and cytoplasmic; multiple bacterial targets also contributes to silver's broad-spectrum activity[34, 57, 63-64]. In reported cases of increased silver resistance, the main determinant involves a periplasmic metal-binding protein, a chemiosmotic efflux pump, and ATPase

efflux pump[65-66]. These plasmid-encoded pumps, which actively transfer the Ag^+ out of the cell, are thought to be a major cause of silver resistance[65-66]. The development of silver resistance is not widespread, which can be attributed to the broad-spectrum activity and the proposed mechanisms, which target multiple bacterial components[63]. Although resistance to silver is a possibility, the rate of development appears to be slower than alternative antimicrobial agents, which gives promise to future development of silver-based antimicrobial therapies in combinatorial and mixed-therapy applications[67]. However, one of the main limitations to using silver as an antimicrobial agent or in combination approaches has been the limited solubility of pure silver metal in aqueous solutions[46]. Our previous work and that presented here show a viable strategy for developing silver-based coatings that circumvent the solubility issue through the use of silver oxide.

Coating implants is a widely investigated method of reducing bacterial contamination following orthopedic surgeries. The complexities of these surgeries, which are often complicated by trauma-related injuries, have yielded a number of different strategies for controlling infection both during treatment and post-surgery. One of the most common treatments in traumatic injuries is the use of antibiotic-loaded bone cement, which is commonly used to fix implants and release a large burst of antibiotics to the localized area in order to prevent infections. Due to the amount of antibiotic loaded into the cement, after the initial burst, the release occurs slowly and over a prolonged period of time; prolonged exposure to antibiotic dosages below the inhibitory concentration is a large contributing factor to the spread of antibiotic resistance[68-69]. The Ag_xO-based coatings described in this work, if applied to a surgical or medical device,

would maintain the antibacterial activity seen in the traditional antibiotics in bone cements, while decreasing the resistance development threat[70]. In addition, the silver oxide coatings are capable of being applied to a wide variety of surfaces and devices not limited to bone cement. The release profiles of silver in complex environments (Figure 6) indicate that sufficient silver will be released to be clinically viable as an antimicrobial in a wound site, as opposed to the amount used in nanoparticle studies[71] 0.35 ppm – 1.12 ppm in our study, compared to 60 ppm - 250 ppm Ag nanoparticles.

Silver nanoparticles have also been commonly used as an efficacious and practical way to coat surfaces; recent advances in nanotechnology have afforded the ability to vary the size of the particles, and the physical characteristics of the particles, and the of the dissolution/elution profile[72]. However, nanoparticle coatings have a distinct set of limitations, based on the fabrication methodology, including inherent variability in material composition. The use of nanoparticles has also shown variability in their toxicity profile, due to the variability in material composition[73-74]. Nonetheless, nanoparticles do provide a straightforward route to biologically active silver, although this route is often confounded by variability in elution rates, the mechanical properties of the nanoparticles, and the ability to adhere the nanoparticles to surfaces.

The majority of recently reported work utilizing Ag^+ compounds as antimicrobials incorporates the use of nanoparticles; in fact, 30% of total nano-products are nano-silver particles[60]. Nanoparticles have become a popular alternative material for the creation of antimicrobial coatings on medical devices and bandages. Although copper, zinc, titanium[75], magnesium, gold[76], and alginate[77] have all been tested for activity, silver nanoparticles have proven the most efficacious against a wide range of bacteria and

viruses[72]. When three types of nanoparticles were compared in a growth curve analysis to $AgNO_3$ as a positive control, only the highest concentrations of both colloidal and biogenic nanoparticles were able to inhibit growth comparable to the positive control in both Gram-positive and Gram-negative bacterial species[78]. Concentrations of Ag^+ the aforementioned study ranged from 0.47 µg/mL – 0.53 µg/mL, with the lowest of those showing no antimicrobial activity[78]. In comparison, the concentrations in the study presented here ranged from 0.35 µg/mL – 1.12 µg/mL, and showed comparable antimicrobial efficacy for both Gram-positive and Gram-negative species at 0.52 µg/mL (equivalent to 30 minutes of release in LB).

Numerous studies have shown that nanoparticle delivery of Ag^+ is more toxic to mammalian cells than delivery via Ag-coated biomaterials[79-80]. Therefore, novel methods for coating biomaterials with various Ag compounds in order to control Ag^+ release have been investigated[57, 81]. Numerous *in vitro* and *in vivo* studies have recently been performed using various Ag-coated materials and have demonstrated antibacterial efficacy in the absence of mammalian cell cytotoxicity[82-88]. Our *in vitro* cytotoxicity results demonstrate that our coatings show cytotoxicity only in a portion of the cell population at 48 hours (Figure 8). Microscopic analysis demonstrated that toxicity was apparent in the cells immediately surrounding the disc and not cells located distally, suggesting that that the local concentration of Ag^+ is higher than the rest of the culture (data not shown). Preliminary *in vivo* results show that subcutaneous implantation of the Ag_xO-coated titanium discs in mice does not result in a detectable increase in Ag^+ in blood compared to controls up to 21 days (data not shown). Collectively, these data suggest that in a "closed system", such as a tissue culture plate, that accumulation of Ag^+

ions can become cytotoxic, which was also suspected by another group in their model system[87]. However, in an "open system", such as an animal, removal of Ag^+ from the local environment via circulation can reduce or eliminate cytotoxic effects. Additional *in vivo* experimentation to investigate the toxicity of these particular coating compositions is warranted.

Previous work has shown that Ag_xO coatings created via reactive sputtering methodologies are vastly superior to nanoparticle materials with regard to uniformity of coating morphology, and exhibit a significantly higher elution rate of silver[57, 89]. The elution rate is the key determinant of antimicrobial efficacy, as silver concentration in solution causes bacterial cell death or bacterial growth arrest[32]. This was confirmed by ICP-MS experiments that were linked to bacterial growth assays (Figures 3, 5, and 7). The results presented here clearly show that the amount of Ag^+ released from the coatings is linked to the antimicrobial activity, and our initial results indicate that the Ag^+ concentration in solution is also linked to the bactericidal vs. bacteriostatic mechanism of action of Ag^+ (Figures 5 and 12). The results indicate that ~3.24 μM Ag^+ in solution is sufficient to exert bactericidal activity against *E. coli*. This is a lower concentration when compared to published reports stating that 18.9 μM Ag^+ is required for complete inhibition of growth[90]. On the other hand, our data shows that even at the highest final concentrations (10.38 μM Ag^+ – 4h time point), silver was acting as a bacteriostatic agent against the Gram-positive species, *S. aureus*. This bacteriostatic activity is in agreement with several reports in the literature, however the mechanism of bactericidal vs. bacteriostatic activity was not reported in any of the publications where Ag concentration was directly measured[91-93].

The difference in bacterial response to Ag^+ in both Gram-negative and Gram-positive bacterial species is evident in the work presented, yet has been previously studied in an attempt to better understand silver's antimicrobial mechanism. When strains of *S. aureus* and *E. coli* were exposed to Ag^+, a cellular stress response led to the condensation of DNA into the center of the cell, cell membrane detachment from the cell wall, cell wall damage, cell shrinkage, and dehydration for both strains[94]. Although damage to the cells appeared similar, *E. coli* (Gram-negative) sustained more extensive structural damage than *S. aureus* (Gram-positive)[94]. Hypotheses for reduced susceptibility of Gram-positive bacteria to Ag^+ are rooted in the composition of the cell wall of Gram-positive bacterium, which is slightly more negatively charged due to a larger presence of peptidoglycan, and therefore thought to trap some Ag^+ in the cell wall[95]. Observations from various studies were confirmed in the data presented in Figures 5 and 12; Ag^+ induces a bacteriostatic effect in Gram-positive bacteria, and a bacteriolytic effect in Gram-negative bacteria[94, 96-98]. While bacteriostatic agents leave the infectious particles intact, it provides a limitation to increase infection scope, and can provide opportunities for combinatorial approaches to clear the infection, including additional administered therapeutics or allowing time for the host immune system to clear the infection.

Conclusion

In this study, silver oxide was applied to titanium foil to test antimicrobial activity as a proof of concept for medical device applications. The coatings were deposited using a reactive sputtering method that allows the process to be carried out at room temperature, making large-scale manufacturing process and applicability to alternative

substrates viable options for future application[46, 57]. In addition, the sputtering method can be adjusted to produce variability in coatings including chemical composition and adjustable elution rates[46, 57, 99]. Coatings can be developed and tailored via composition changes or the creation of distinct, multi-layered systems in which each layer of the coating has different chemical compositions and/or elution profiles for Ag^{+}. In addition to the layering capability, homogeneous coatings of varied chemical compositions can also be used to modulate elution profiles.

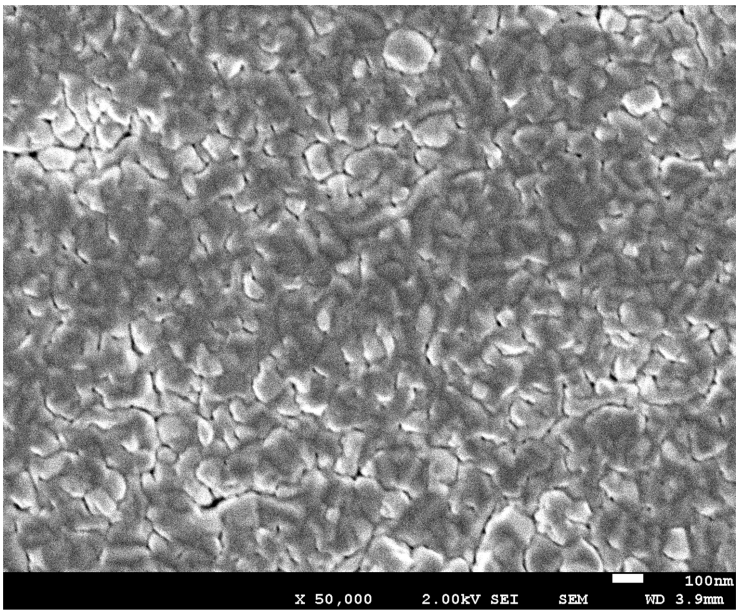

Figure 2. SEM image of a mixed phase sample of silver oxide deposited at 20 mTorr in a 67/33 mixture of Ar/O_2 on a titanium foil substrate. This film is approximately 500 nm thick.

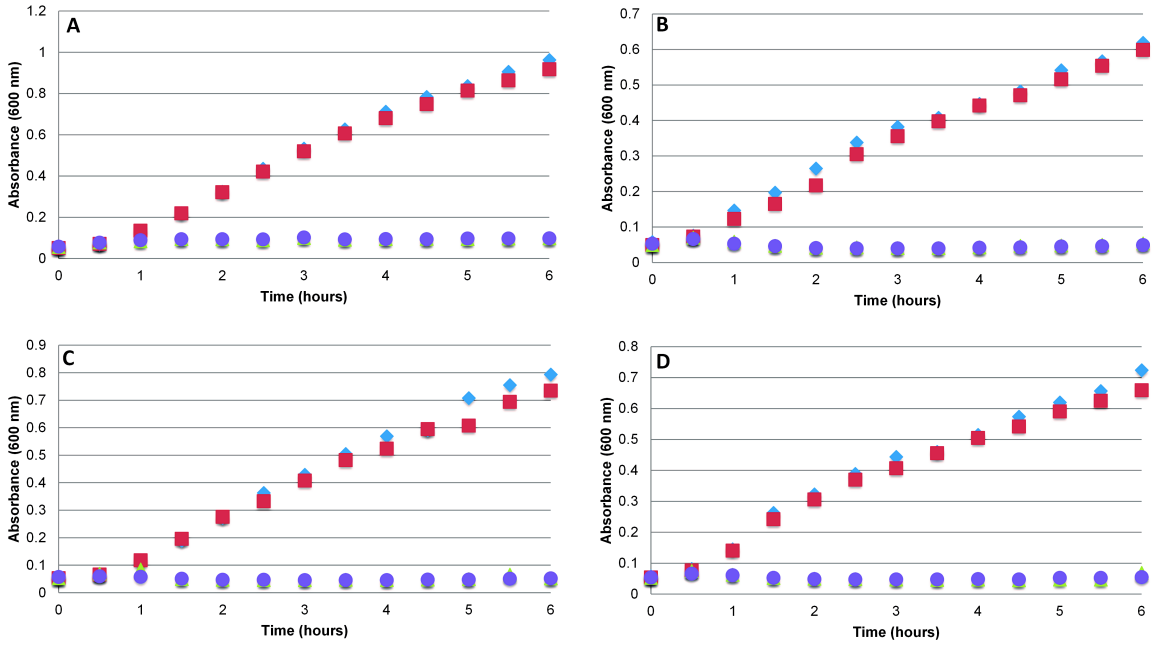

Figure 3. Antibacterial activity of Ag_xO coatings in liquid culture. Ti or Ti coated with Ag_xO (~150 nm double-sided) discs were added to cultures of (A) *S. aureus* (starting density ~3.93 x 10^6 CFU/mL), (B) *E. coli* (starting density ~3.73 x 10^7 CFU/mL), (C) *P. aeruginosa* (starting density ~3.53 x 10^7 CFU/mL) and (D) *K. pneumoniae* (starting density ~3.43 x 10^6 CFU/mL). Symbols are (▲,●) for Ag_xO-coated discs, (u) for untreated control, and (n) for uncoated titanium disc control.

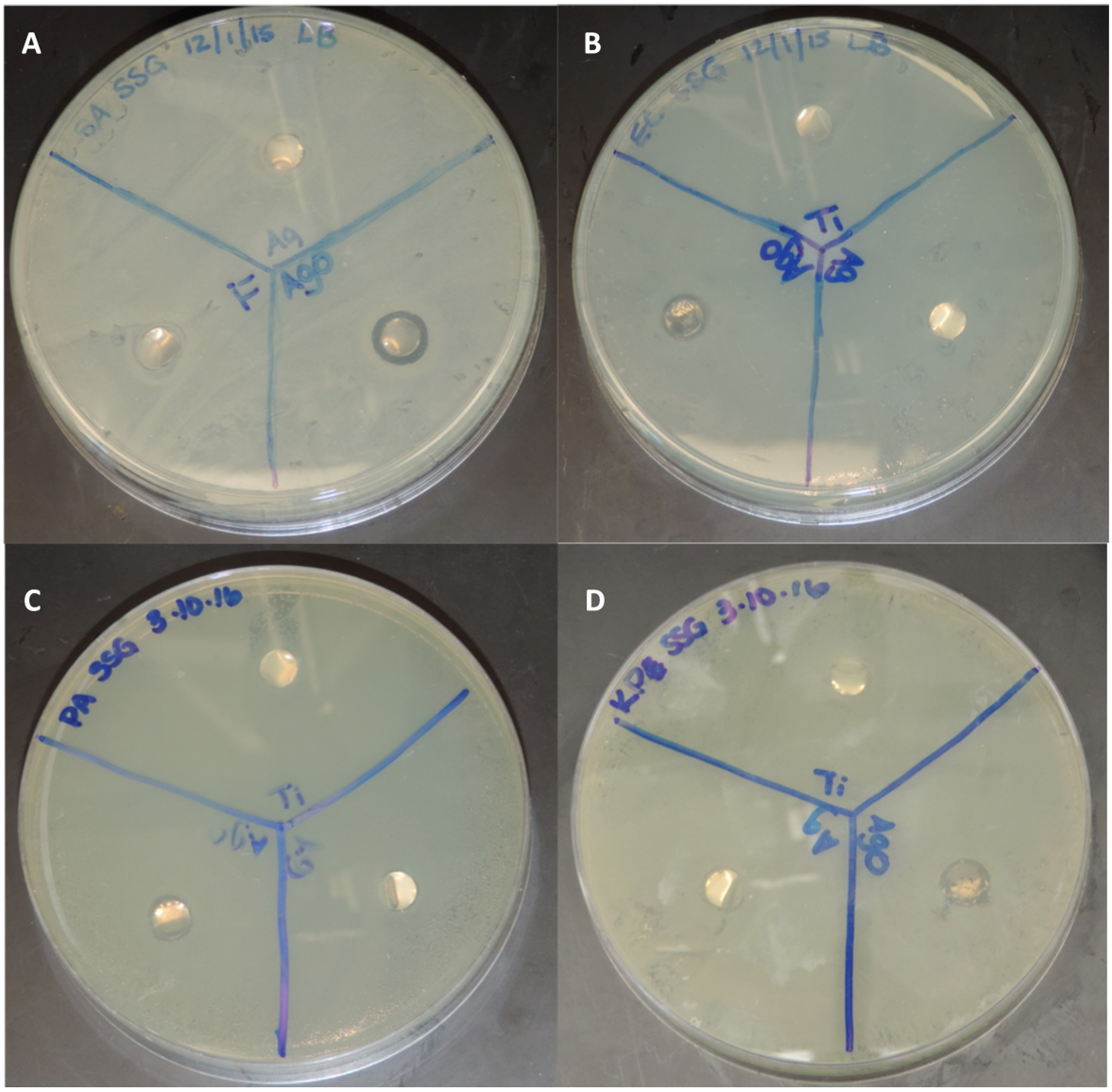

Figure 4. Zone of inhibition assay. Images of LB plates seeded with, (A) *S. aureus* (B) *E. coli*, (C) *P. aeruginosa*, and (D) *K. pneumoniae*. The Ag_xO disc (labeled AgO on the plates) exhibited ZOI of (A) 0.9 cm for *S. aureus,* (B) 1 cm for *E. coli,* (C) 0.8 cm for *P. aeruginosa*, and (D) 0.8 cm for *K. pneumoniae*. Diameter of the disc in each case is 6.5 mm (1/4"). No ZOIs were evident for Ag-coated or Ti control discs.

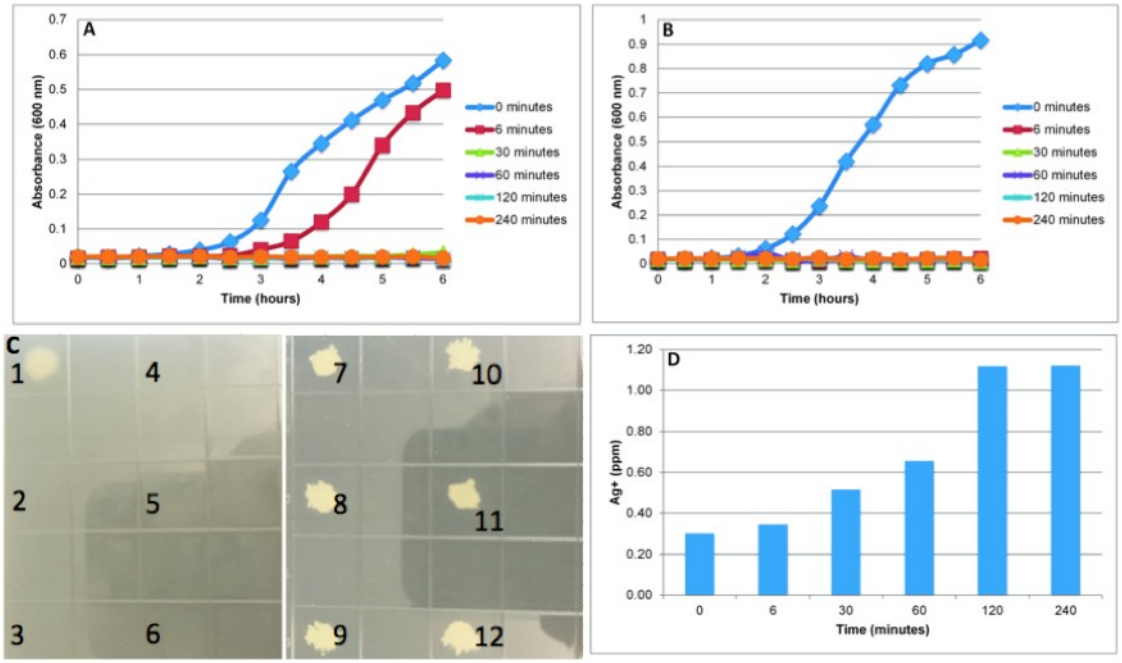

Figure 5. Growth curve analysis in media pre-conditioned by exposure to Ag_xO coated (150 nm, double-sided, 1/4") discs. (A & B) Data shown are (a) *S. aureus* at an initial density of ~$1.22x10^5$ CFU/mL and (b) *E. coli* at an initial density of ~$1.34x10^6$ CFU/mL. (C) Plating of aliquots of cultures from the 3h time point on LB agar plates (*E. coli* shown in 1-6, *S. aureus* shown in 7-12); time stations as follows: 0 min. spots 1,7; 6 min. spots 2,8; 30 min. spots 3,9; 60 min. spots 4,10; 120 min. spots 5,11; 240 min. spots 6,12; (D) ICP-MS analysis of LB media after incubation with Ag_xO discs for fixed time points corresponding to pre-conditioning time points in (A & B).

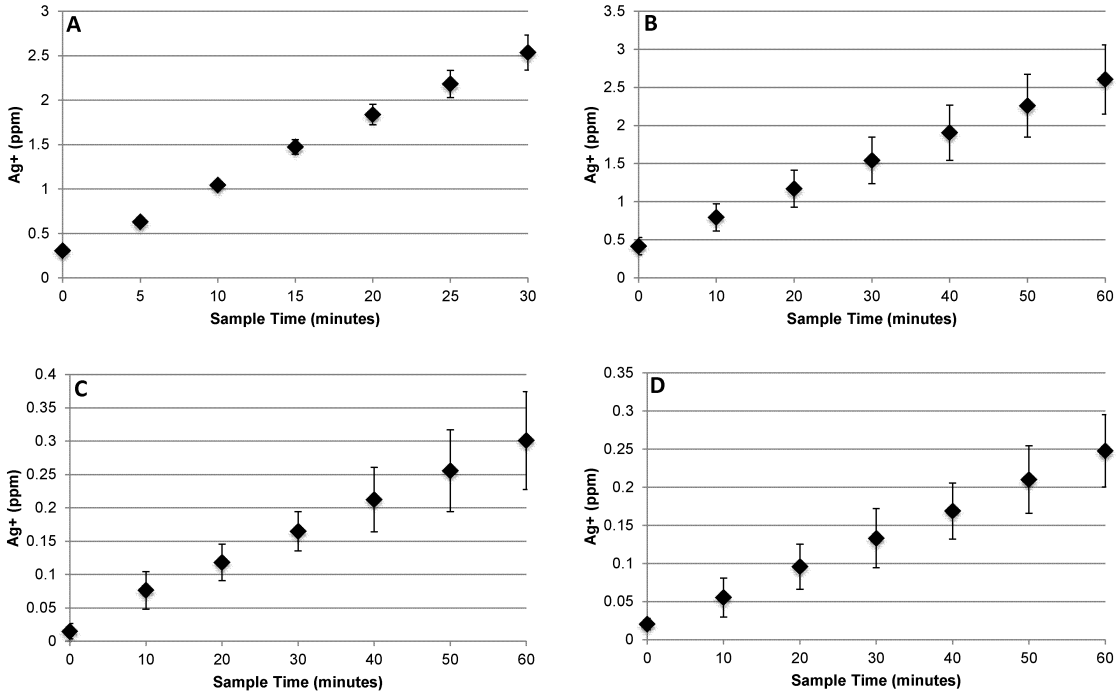

Figure 6. ICP-MS analysis of Ag^{+} released from Ti discs with a single-sided 150 nm thick Ag_xO coating in (A) water, (B) PBS, (C) LB broth, and (D) DMEM for each media type. Data shown are averages of 3 replicates and error bars represent standard deviations. Note the difference in timescale for (A) compared to (B-D).

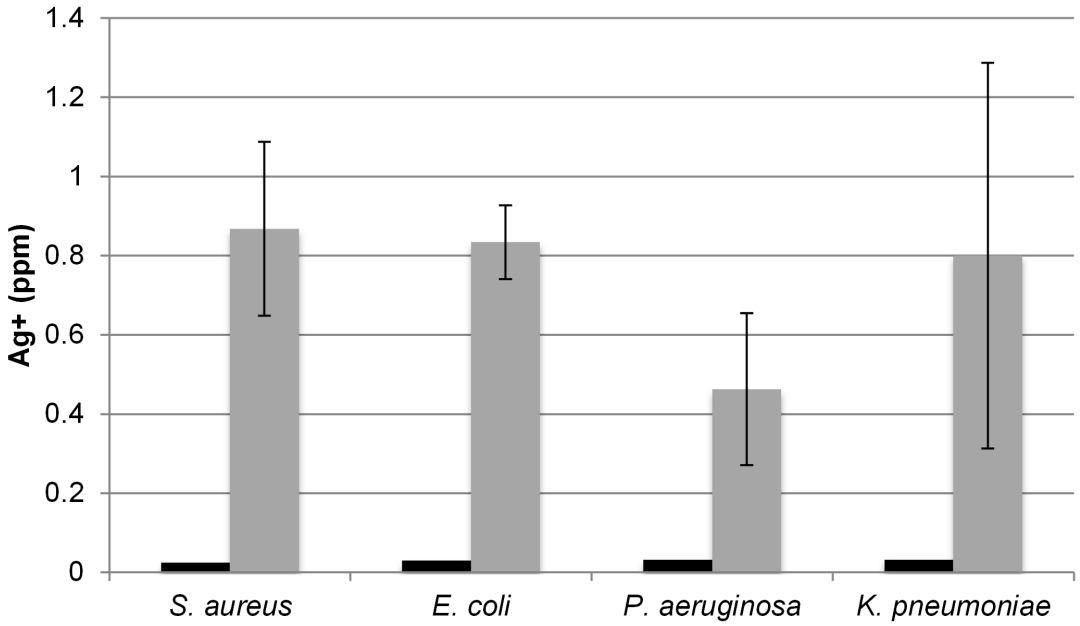

Figure 7. ICP-MS analysis of Ag^{+} from growth curve samples shown in Figure 3. Samples were removed at the end of the 6h time course. Black bars represent samples taken from cultures treated with the uncoated Ti discs while the gray bars represent samples treated with Ag_xO-coated Ti discs. Error bars represent ranges for Ag_xO samples based on the replicate from each bacterial strain.

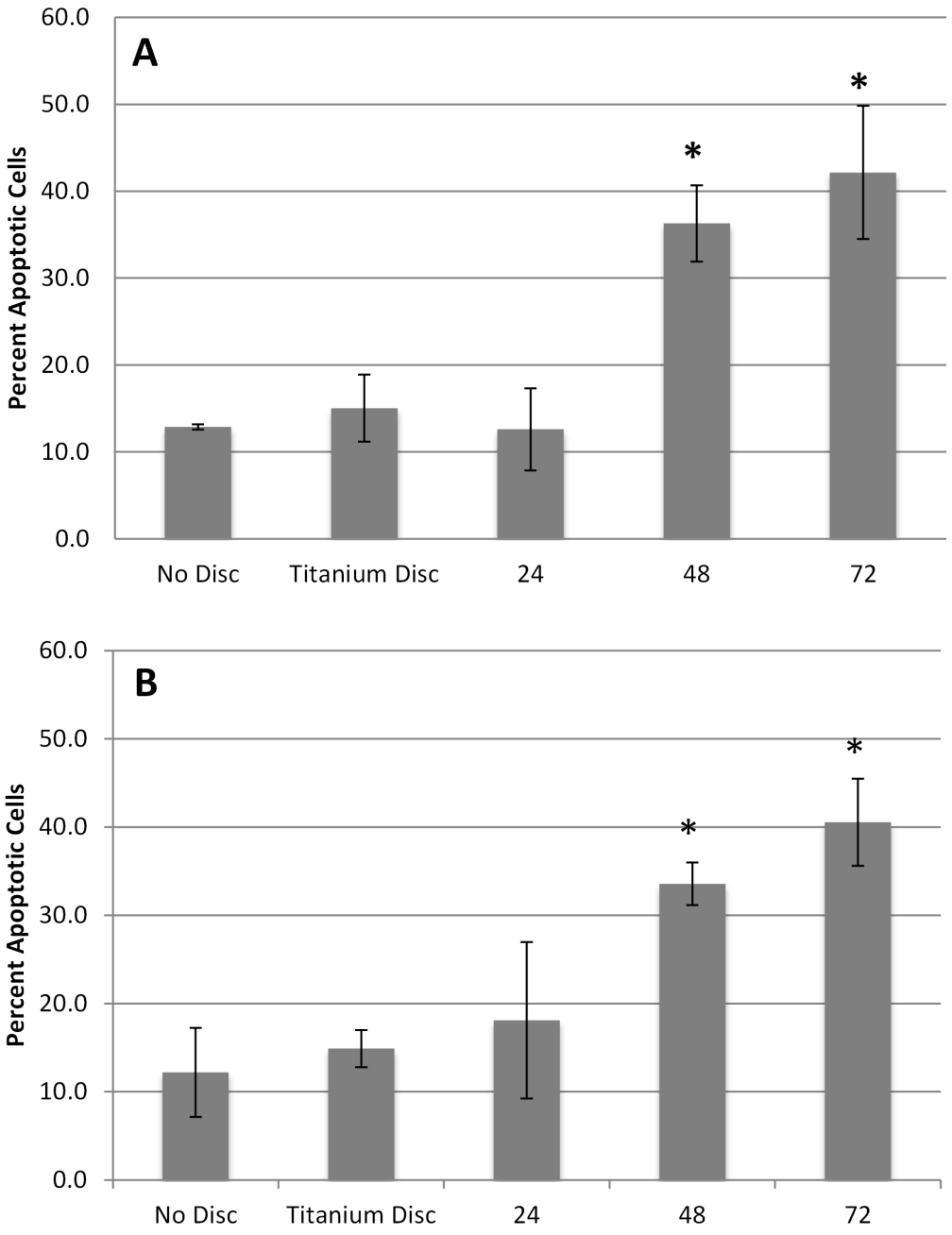

Figure 8. Mammalian *in vitro* toxicity assays. NIH3T3 (1.5 x 10^6 cells) were plated and cultured for approximately 12 hours. Discs were then added for the indicated time points, then cells collected and stained with Annexin-V and PI. (A) ~150 nm coating, double-sided or (B) ~150 nm coating, single-sided discs - all 0.635 cm discs. Assays were performed in triplicate and the averages are graphed with standard deviations. *p-value < 0.05.

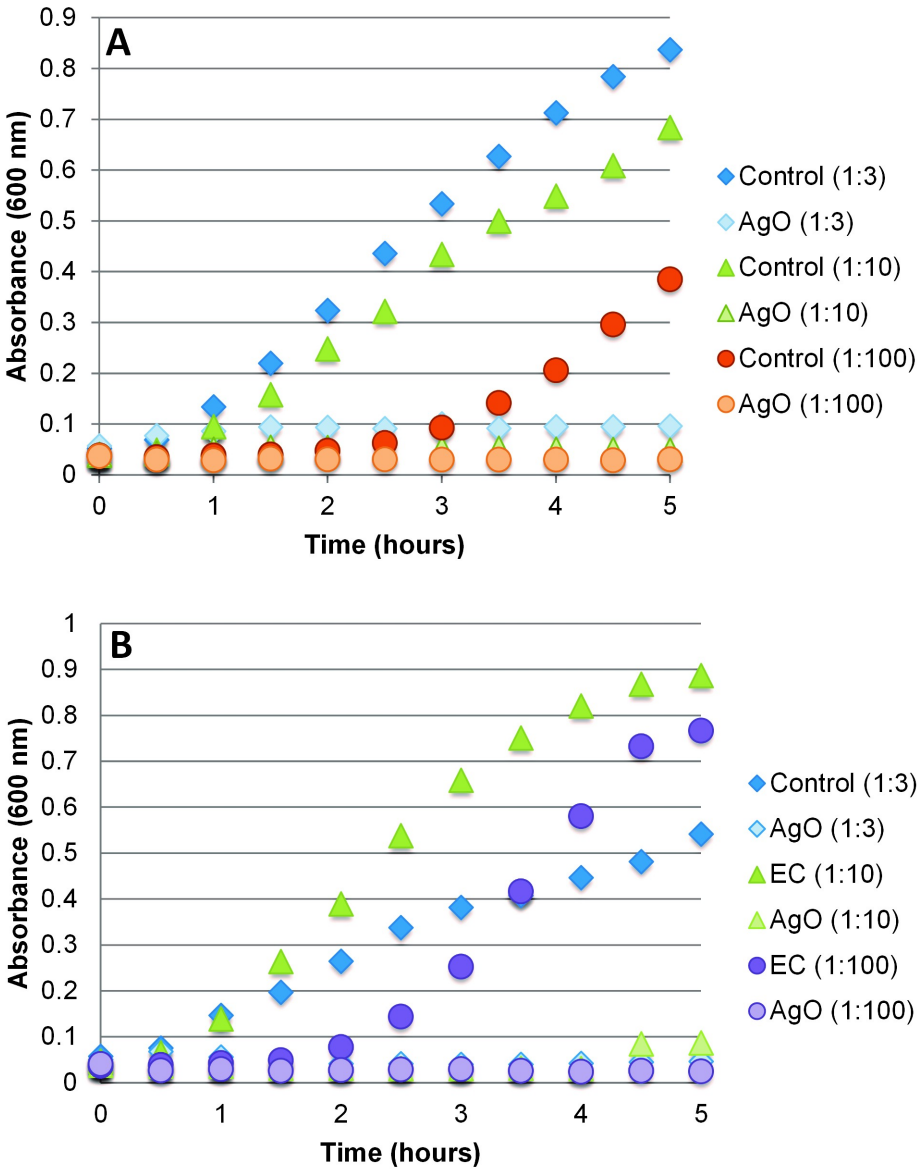

Figure 9. Effect of initial culture density on antimicrobial efficacy. Titanium or titanium coated with Ag_xO (~150nm double sided) discs were added to cultures of (A) *S. aureus* and (B) *E. coli*. Samples indicated are (u) 1:3 dilutions, (▲) 1:10 dilutions, (●) and 1:100 dilutions.

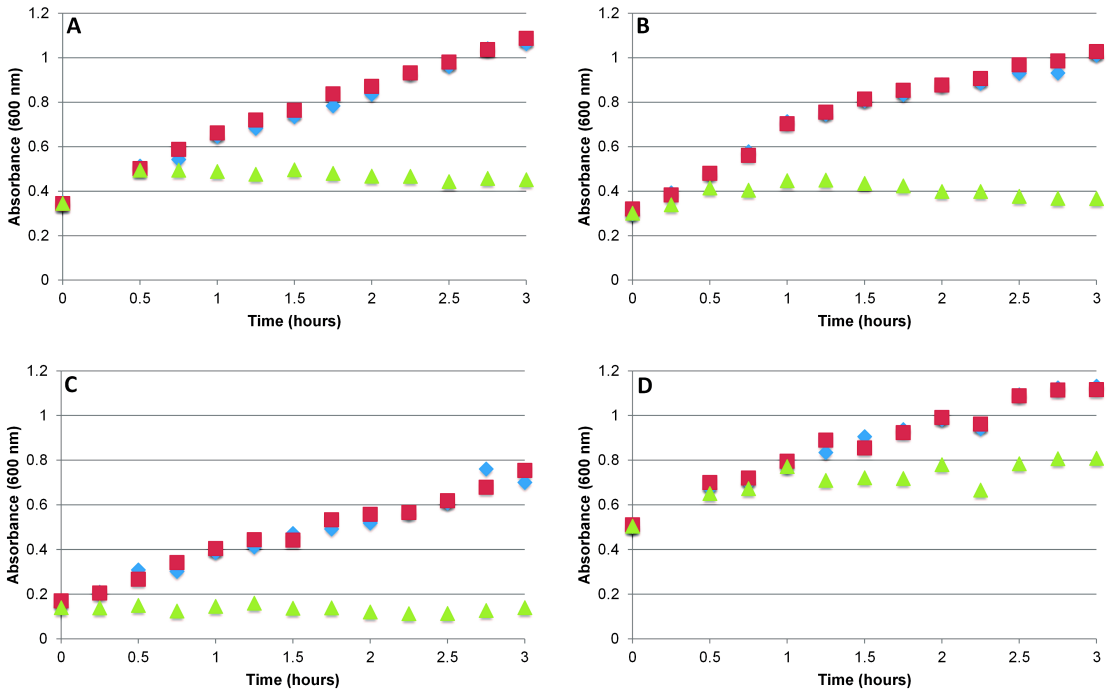

Figure 10. Effect of increased culture density on antimicrobial efficacy. Titanium or titanium coated with Ag_xO (~150nm double sided) discs were added to cultures of (A) *S. aureus* (starting concentration of $3.46x10^6$ CFU/mL), (B) *E. coli* (starting concentration of $3.06x10^6$ CFU/mL), (C) *P. aeruginosa* (starting concentration of $3.70x10^6$ CFU/mL) and (D) *K. pneumoniae* (starting concentration of $5.06x10^5$ CFU/mL) after extended growth before additions. Samples indicated are (p) Ag_xO-coated discs, (u) untreated control, and (n) titanium disc.

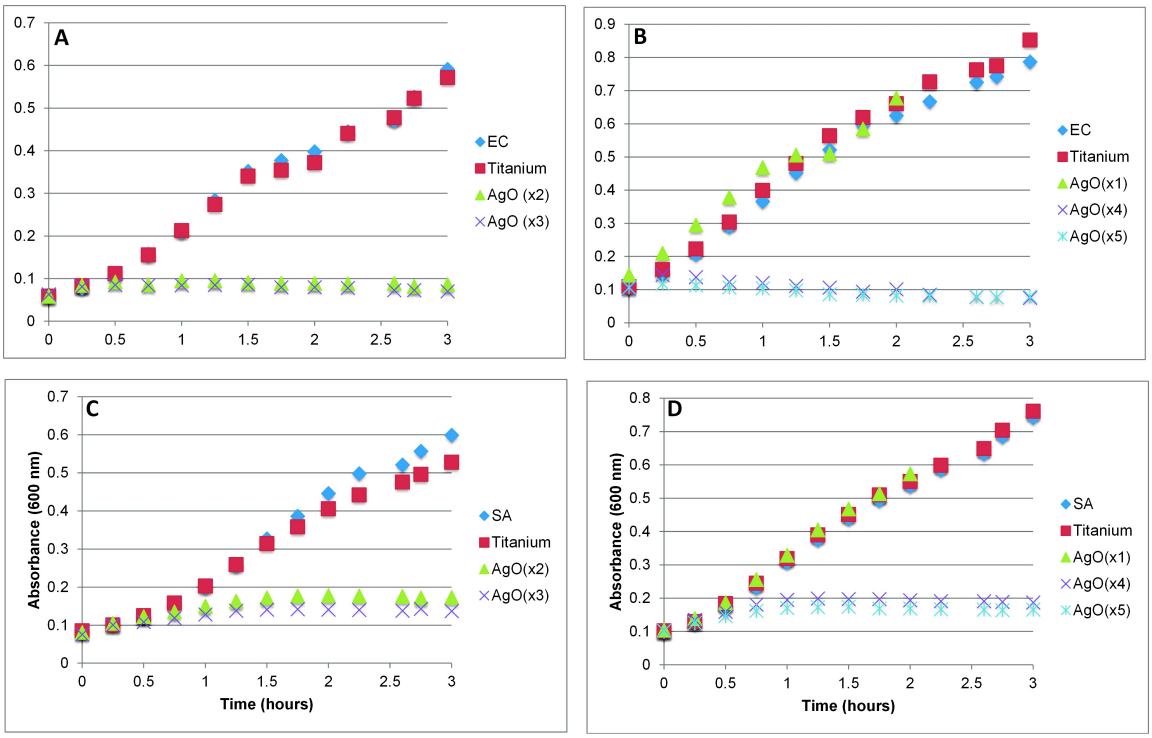

Figure 11. Growth curve analysis using varying numbers of 1/8" Ag_xO-coated test discs for (A) and (B) *E. coli*, and (C) and (D) *S. aureus*. In figures (A) and (B), curves are shown for a single 0.3175 cm piece, as well as up to five test discs in a single tube; in both the cases of *S. aureus* and *E. coli*, adding more discs to the test tube decreased the bacterial concentration in the tube. Bacterial concentrations for *E. coli* experiments ranged from $5.23x10^7$ – $1.07x10^8$ CFU/mL, *S. aureus* concentrations ranged from $6.66x10^6$ - $1.02x10^7$ CFU/mL.

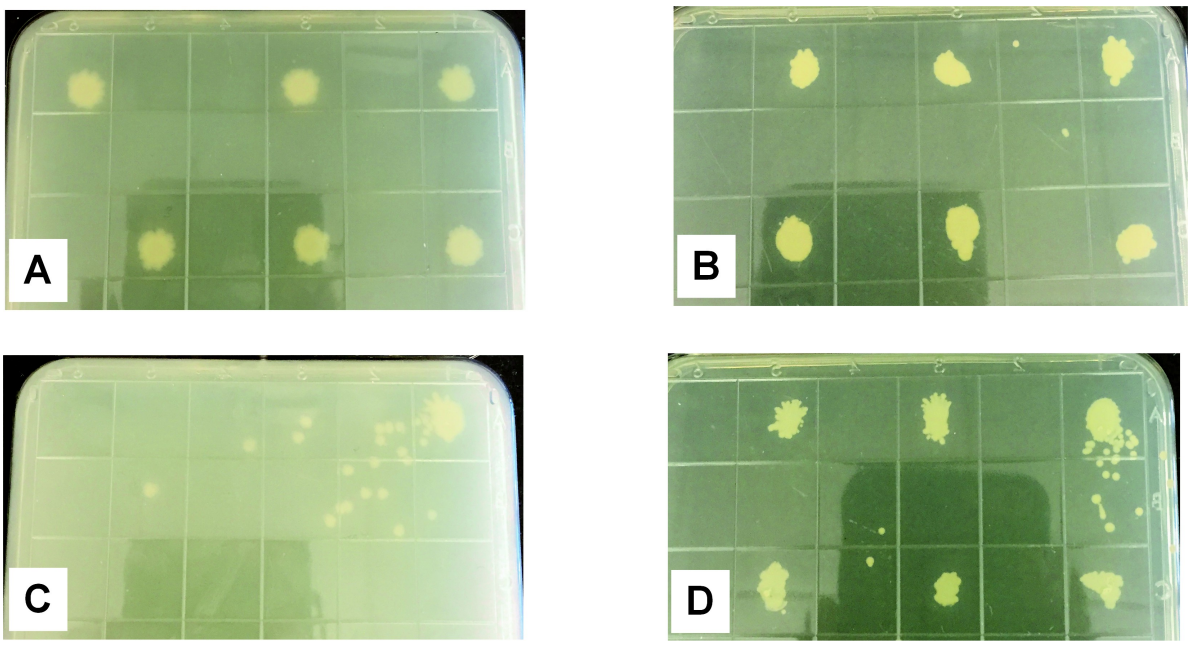

Figure 12. Spot platings for both bacterial species at varying time points during the pre-conditioned media assay. *E. coli* is represented at (A) 0 hours, and (C) 6 hours, while *S. aureus* is shown at (B) 0 hours and (D) 6 hours.

Table 1.

Ag^+ Elution Rates in Various Types of Media.

Media Type	Elution Rate (ppm/min)			R^2 Value
Water	7.55E-02	±	0.00711	1
LB Broth	4.55E-03	+	0.00107	1
DMEM	3.65E-03	+	0.000608	1
PBS	3.34E-02	+	0.00578	1

Note. Calculated elution rates as well as R2 values from a linear fit are shown for each media type. Values were calculated based on three ICPMS runs for each media type.

Chapter 3

Efficacy of Silver Oxide Coatings *In Vivo*

Introduction

As surgical practices have advanced, so has the ability of the medical community to combat surgical complications, including infection (most notably those caused by surgical implants). For years, the instances of infections after orthopedic surgeries were low, yet recent studies have shown that the risk for post-surgical infection is increasing[100]. Antibiotic resistance and the continued ability for bacteria to overcome antibiotic treatment is a likely explanation for an increase in infections in medicine, most notably in healthcare settings[2, 4]. As such, it has become a goal of both the medical and scientific communities to develop alternative treatments to reduce the occurrence of post-operative infections, most of which occur on the surface of the implant. Targeting bacterial adhesion is a common strategy in preventing biofilm formation, which occurs when microorganisms attach to a surface and embed in a matrix of secreted proteins, nucleic acids and polysaccharides[101]. Biofilms are often more resistant to treatments, and can exacerbate the effects of the infection[102]. In the United States alone, an estimated 1.7 million healthcare-acquired infections each year are caused by biofilms, accounting for $11 billion in healthcare costs[5, 103]; it is estimated by the CDC and NIH that 65-80% of infections can be attributed to biofilms[104].

Silver has been known as an antimicrobial agent for centuries, but its use decreased with the rise in the use of antibiotics in the late 1900's. Yet the rise of antibiotic resistant organisms has renewed interest in the use of silver compounds for this purpose. Silver resistance has been identified, yet the majority of silver resistant bacteria were isolated

from environments in which silver and other metals were naturally-occurring[32] as well as reports in clinical environments and wounds treated with silver nitrate[32]. Upon further research, the silver resistance mechanism was found to be very similar to that of other metal-resistance mechanisms, and in that way, has been widely studied[32, 105]. The primary mechanism of silver resistance is linked to metal efflux pumps, which export silver out of the bacterial cytoplasm[105-106].

Coating orthopedic implants with silver nanoparticles has become somewhat common, yet recent data suggests that silver oxide formulations are more efficacious against microbial organisms, as well as less toxic towards mammalian cells than nanoparticles[55, 79]. The use of coatings at the surface of an implant rather than systemic antibiotic treatment to control post-operative infection is ideal to prevent selection of antibiotic-resistant pathogens.

Preliminary studies were conducted on Ag_xO-coated discs to assess antimicrobial efficacy in solution. It was found that silver coatings eluted Ag^+ from the surface of coated titanium discs in sufficient concentration to kill various bacteria. It was also previously shown that there was limited toxicity against mammalian cells in *in vitro* assays. While useful in determining toxicity of agents, *in vitro* assays are limited in that they are a closed system, which does not accurately recapitulate a dynamic and exchanging *in vivo* environment. In contrast, the mammal is an open system, capable of removing molecules, including silver ions, from a local area to reduce concentration and/or eliminate the molecule from the system.

The goal of this study was to determine the efficacy of Ag_xO-coated titanium discs in preventing bacterial adhesion in a mouse model of infection. This was done by subcutaneous implantation of Ag_xO-coated discs in mice, and subsequent injection of a specified amount of fluorescent bacteria to induce probable infection.

Materials and Methods

Bacterial culturing. Luminescent bacteria, *S. aureus* (Xen-36), *E. coli* (Xen-16), *P. aeruginosa* (Xen-5) (Perkin Elmer, Waltham, MA) were streaked onto LB - Miller agar (Difco) plates from frozen glycerol stocks, grown overnight at 37°C in a non-humidified chamber, and stored at 4°C.

To prepare overnight liquid cultures, a single colony of each bacterial strain was added to 3 mL LB broth (Difco) in sterile culture tubes. Tubes were placed in a shaking incubator at 37°C overnight to allow for sufficient bacterial growth. Following the incubation period, dilutions of the overnight culture were prepared in Muller-Hinton broth (Criterion) 1:100; changing broth provides for better short-term bacterial growth and is comparable to MIC assay protocols.

Bacterial growth analysis. Protocol followed is explained in Chapter 2, Materials and Methods section labeled 'Bacterial culturing'.

ICP-MS analysis. All ICP samples were compared against a standard prepared in 5% HNO_3 containing 1,000 ppm silver nitrate (Ricca) calibrated to fit a linear curve model and containing expected experimental outcome values. Media collected from the *in vitro* toxicity assays was analyzed in order to assess silver content in 5 mL DMEM with a starting concentration of $1.5x10^5$ cells.

For mouse blood sample preparation, approximately 100 µL of blood was collected into a centrifuge tube containing 50 µL of 5% sodium citrate via submandibular bleeding at the indicated times post-surgery. Cells were pelleted at 5,000 RPM for 5 min, and 100 µL of supernatant was added to 3 mL of 5% HNO_3. Samples were then analyzed by ICP-MS in order to determine serum silver concentration.

***In vivo* bacterial adhesion assay**. Mice were anesthetized using 5% isoflurane in O_2 for induction and 1-3% isoflurane in O_2 for maintenance. A 5.5 cm long, 2.5 cm deep incision was made on the back flank of mice and a subcutaneous "pocket" created. A Ag_xO-coated or titanium uncoated 1 cm x 2 mm titanium disc was inserted into the "pocket" and the incision closed with surgical staples. PBS or one of three luminescent variants of clinically relevant pathogens, *S. aureus*, Xen-36 (10^5 CFU), *E. coli,* Xen-16 (10^7 CFU), and *P. aeruginosa,* Xen5 (10^5 CFU) (Perkin Elmer), were then introduced into the area near the surgical "pocket" by subcutaneous injection of the biomaterial using a needle for precision. Temperature and body condition of the mice were monitored daily.

Results

Effect of silver-coated discs on bacterial growth. Ag_xO coatings were previously tested on non-luminescent varieties of common healthcare-acquired bacterial strains to determine coating thicknesses and efficacy in solution (Chapter 2). Luminescent bacterial strains were used to provide the option of imaging the mice to observe the infection, as well as obtaining luminescent readings for bacterial cultures

after the disc removal. Previous experimentation confirming the antimicrobial efficacy of the test discs was performed with non-luminescent bacterial strains.

Figure 13 shows the growth curves of various luminescent bacterial species (*S. aureus, E. coli, P. aeruginosa* - provided by Perkin Elmer) in the presence of a titanium disc, or a 150nm Ag_xO coated double-sided disc, one replicate made from two different batches. (Double-sided discs are coated with the indicated silver formulation on both sides of the disc; single-sided discs are only coated on one side.) The cultures containing the coated discs exhibited growth inhibition when compared to the control culture and the titanium cultures, as well as reproducibility between batches. The results from this experiment match previously reported data, as outlined in Chapter 2.

Toxicity of Ag_xO coatings in NIH3T3 cell lines. Previous results demonstrated that exposure to either a 150nm double- or single-sided disc induces apoptosis of NIH3T3 cells in culture. Figure 14 shows that silver ions consistently eluted from the discs (both double sided, A, and single sided, B) over the course of the experiment. Importantly, silver ion concentration continued to rise in the media over the time course examined (data not shown).

Establishing the *in vivo* bacterial adhesion assay. In order to determine whether Ag_xO coatings can limit or reduce bacterial infection *in vivo*, a mouse model of infection was established. Mice were anesthetized and injected with buprenorphine; titanium discs were then placed subcutaneously, the wound was closed using surgical staples, and the mice were injected subcutaneously with PBS or a culture of a luminescent bacterial strain, as indicated. Mice were live-imaged at various points post-surgery to visualize

luminescent bacteria and X-ray imaging was performed to visualize the mice. Bacteria could be detected *in vivo* by 4 days post-surgery (Figure 15A, 15C, 15D). However, the immunocompetent mice were able to clear the infection by 2 weeks (Figure 15B). Pilot studies were performed with immunocompromised mice under the supervision of the attending veterinarian; regular monitoring of the mice indicated hypothermia in a high number of infected animals, which required immediate euthanasia to prevent imminent death[107]. Therefore, all subsequent experiments were performed in immunocompetent mice with 2-4 days of infection. Discs were retrieved from euthanized mice and cultured in LB to determine the presence of bacteria (Figure 15E); OD_{600} and luminescence measurements demonstrate that the bacteria adhering to the disc are the injected luminescent bacteria and not an opportunistic infection (Figure 15F).

Determining the safety of Ag_xO-coated discs *in vivo*. *In vitro* studies suggested that Ag_xO-coated titanium discs are toxic to mammalian cells, as reported in Chapter 2. Of note, it appeared that the cells closest to the disc died first, while those distal to the disc did not show signs of apoptosis by 72h (data not shown). These data suggest that the local concentration of silver ions may be high enough to induce apoptosis in a closed system. However, this is not indicative of an *in vivo* system, since animals are capable of clearing silver ions from the local area and excreting them from the organism. Therefore, whether Ag^+ can be detected in the serum of mice implanted with Ag_xO-coated discs was evaluated. Figure 16 shows that there were no detectable increases in silver ion concentration in mice implanted with Ag_xO-coated discs compared to control mice implanted with an uncoated titanium disc. Interestingly, there was no indication of tissue damage in mice implanted with the Ag_xO-coated discs up to 21 days post-surgery

(Figures 17B and 17C) as compared to those implanted with titanium controls (Figure 17A). However, long-term toxicity studies will have to be performed in order to determine the feasibility of using Ag_xO formulations in the clinic.

Discussion

Overall, the experimental results presented show the ability of Ag_xO-sputtered discs to inhibit luminescent bacterial growth, as well as their limited toxicity in cellular culture. Observed toxicity was confined primarily to the immediate area surrounding the disc, suggesting that testing in a closed system is not indicative of *in vivo* results. In addition, *in vivo* testing produced an infection model in immunocompetent mice as well as methodology to remove and quantify bacterial adhesion on the implanted disc. When blank discs were replaced with Ag_xO discs in the mouse bacterial adhesion model, blood samples were removed from test animals and silver concentrations were found to be similar in both the control subjects and test subjects three weeks post-surgery.

In vitro experiments demonstrate that Ag^+ eluting coatings do result in some level of toxicity to mammalian cells. The antimicrobial activity is directly linked to Ag^+ concentration in solution, and reports in the literature indicate that silver ion concentration can result in mammalian cell toxicity[61, 108]. To address the concentration-toxicity relationship, we analyzed silver concentrations by ICP-MS from *in vitro* cell culture experiments (Figure 14). When compared, the single-sided discs (Figure 14B) produced silver concentrations approximately half that of the double-sided discs (Figure 14A), and at all time points including Ag_xO-sputtered discs Ag^+ content was relatively equal, indicating that at 24h the culture has reached saturation. As reported previously,

the double-sided discs had a reported maximum toxicity of approximately 40% at the 72h time point (Chapter 2) and an average Ag^+ content of 8.63 +/- 0.333 ppm. In the same respect, the single-sided discs had a reported maximum toxicity of approximately 36% at the 48h time point and an average Ag^+ content of 3.68 +/- 0.691 ppm. In both cases, the apoptotic cells were located in immediate proximity to the test disc, indicating that in open systems, toxic effects may be minimized. When compared to a similar study, silver nanoparticles were used to determine both IC_{50} and total lethal concentrations of Ag^+ in NIH3T3 cells; these concentrations were found to be 72 ppm and 86 ppm, respectively[61]. When compared to the experimental values, even the higher concentration, double-sided discs were eight times below the LC_{50} value.

In an effort to extend the *in vitro* toxicity studies to an *in vivo* system, both immunocompetent and immunocompromised mice were implanted with uncoated titanium discs and injected with various luminescent bacterial strains. Mice were imaged to further identify the scope of any bacterial infections, although in some cases, evidence of infection was observed before imaging. Figures 15A and 15B show mice infected with *S. aureus*, in which half of the test mice were able to clear the infection before imaging (Figure 15B). The optimal imaging period was determined to be 2-4 days in the immunocompetent model for *S. aureus*, *P. aeruginosa* (Figure 15C) and *E. coli* (Figure 15D) mice. None of the immunocompromised mice were imaged; shortly after surgery, the majority of infected mice showed symptoms of hypothermia indicating likely systemic infection and imminent death, so the mice were euthanized and experiments with immunocompromised mice discontinued. Further investigation in immunocompromised models will require an adjusted bacterial load and a different

immunocompromised mouse model. Following imaging, discs were extracted and cultured at 37°C overnight in order to quantify bacteria (Figure 15E). OD_{600} and luminescent measurements were performed on the cultures (Figure 15F); luminescence confirms that the bacteria attached to the disc are the injected bacteria and not an opportunistic infection. Culturing of the implanted discs confirms that the bacteria were viable, as well as reinforces the previous findings that the effects of Ag_xO on *E. coli* is bactericidal, while *S. aureus* is bacteriostatic.

There are various *in vivo* models that can be utilized to study infection, including non-mammalian models, such as *C. elegans*[109]. For the purposes of these studies, it was concluded that a mammalian model, mice in particular, would yield the most translatable data. There are numerous infection models that can be employed in mice, including central venous catheter models, subcutaneous foreign body infection models, intraperitoneal foreign body infection models, urinary tract infection models, ear, nose and throat infection models, respiratory tract infection models, and osteomyelitis infection models[109]. The subcutaneous foreign body infection model was utilized in these studies, as this is the least invasive and least technically challenging of the models indicated above. In addition, this is the best system out of those listed above for inserting the coated discs that have been utilized in this study thus far. For example, the coated discs could not be inserted in an intraperitoneal foreign body infection model. In the future, it is possible that additional systems will be utilized. For example, coating of catheters and using the urinary tract infection model or the central venous catheter model may be utilized.

Following the previously established protocol, Ag_xO-sputtered discs were inserted into mice to assess toxicity and Ag^+ levels in the blood. Following blood draws at various time points post-surgery, ICP-MS analysis of samples obtained from mice containing uncoated Ti discs and Ag_xO sputtered Ti discs confirmed that there was no difference in silver content in the blood between both groups. This confirms the ability of silver to be readily removed from the body in an open system. Extensive studies have been completed on the oral toxicity of silver in both murine and rat models, which provide some insight into the levels of silver ions that cause systemic toxicity in each model. Following oral doses of silver nanoparticles in a murine model, silver was detected nearly system-wide, in the liver, kidneys, brain, skin, pelt, spleen, eyes, muscles, blood, small intestine, stomach, lungs, bladder, prostate, tongue, teeth, salivary glands, thyroid, parathyroid, heart, pancreas and duodenum[44, 79, 104, 110-120]. In a separate study conducted with rats, tissue accumulation of silver was found to be dose-dependent following an initial oral dose[80]. Further experimentation is required to assess if subcutaneous administration of silver will yield a similar system-wide presence in a murine model, as well as if certain organs will be more affected by the presence of silver than others.

Conclusion

Follow-up experiments are currently demonstrating that the coatings are more efficacious against Gram-negative compared to Gram-positive bacteria. These results are consistent with previous results showing the tendency for AgO to be bacteriostatic to Gram-positive and bacteriolytic to Gram-negative bacteria. Additionally, further experimentation in the murine infection model should provide further insight into the excretion methods of silver from the body, as well as potential specific organ toxicity.

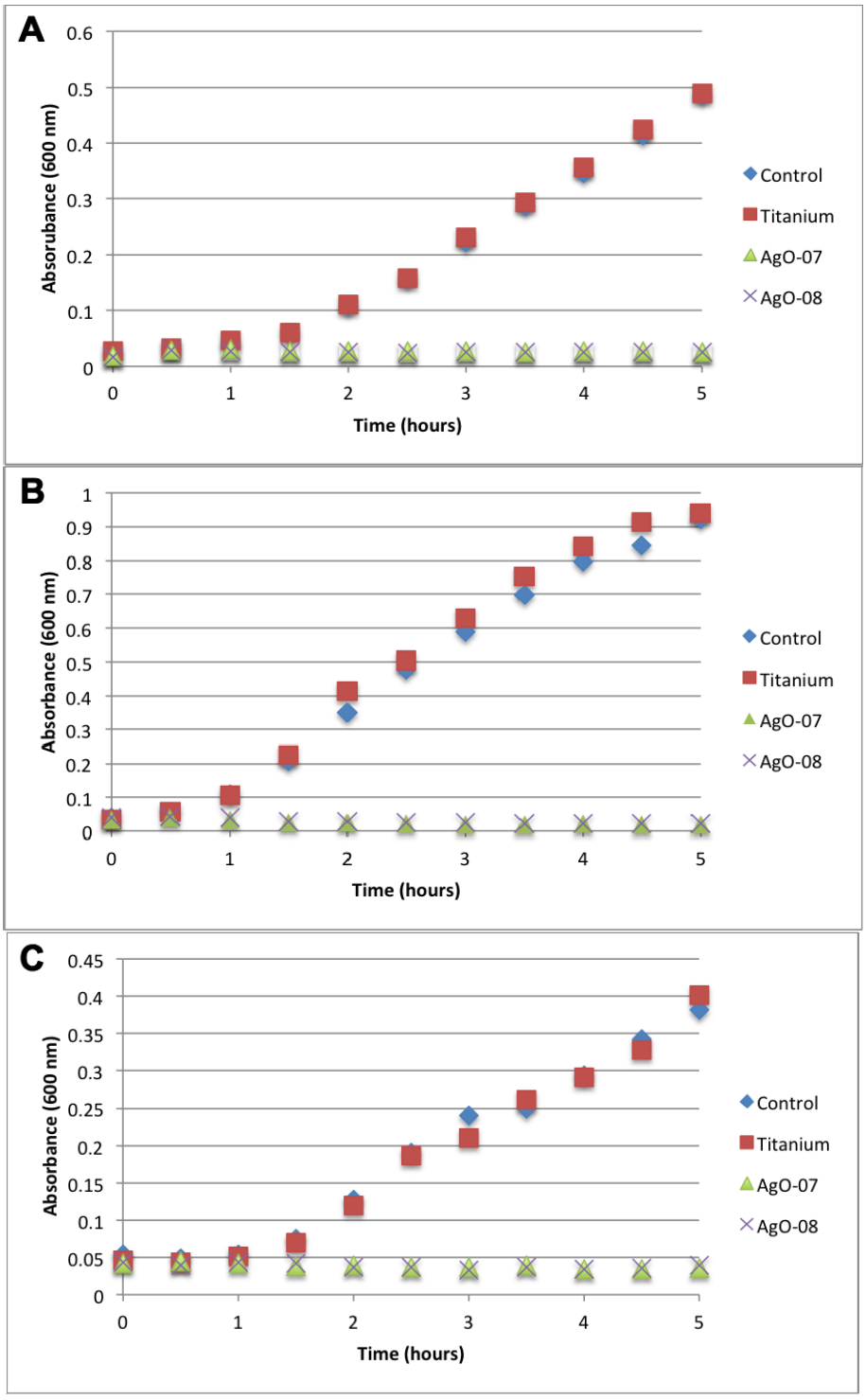

Figure 13. Effect of initial culture density on antimicrobial efficacy. Titanium or titanium coated with ~150nm Ag_xO double-sided discs were added to cultures of (a) *S. aureus* (Xen-36) (starting concentration: $1.10x10^5$ CFU/mL), (b) *E. coli* (Xen-16) (starting concentration: $2.13x10^6$ CFU/mL), and (c) *P. aeruginosa* (Xen-5) (starting concentration: $1.71x10^6$ CFU/mL).

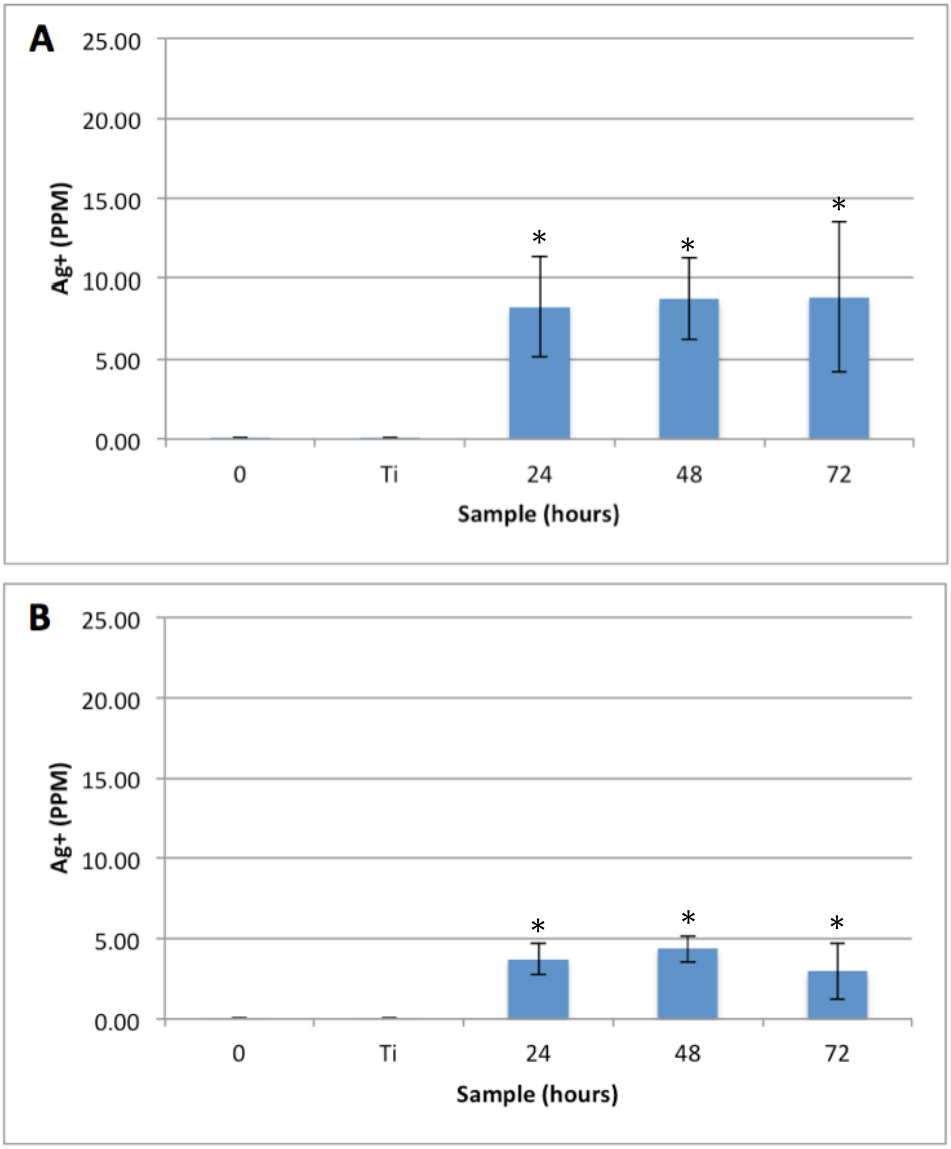

Figure 14. Silver concentration following exposure to various discs and times. Uncoated or Ag_xO coated titanium discs, (a) 150nm double-sided or (b) 150nm single-sided, were added to $1.5x10^6$ NIH3T3 cells in a 6-well plate for the indicated times and cellular toxicity determined by Annexin-V assay. Media was collected at each time point and analyzed by ICP-MS for silver ion concentration. Assay was performed in triplicate. *p-value < 0.05.

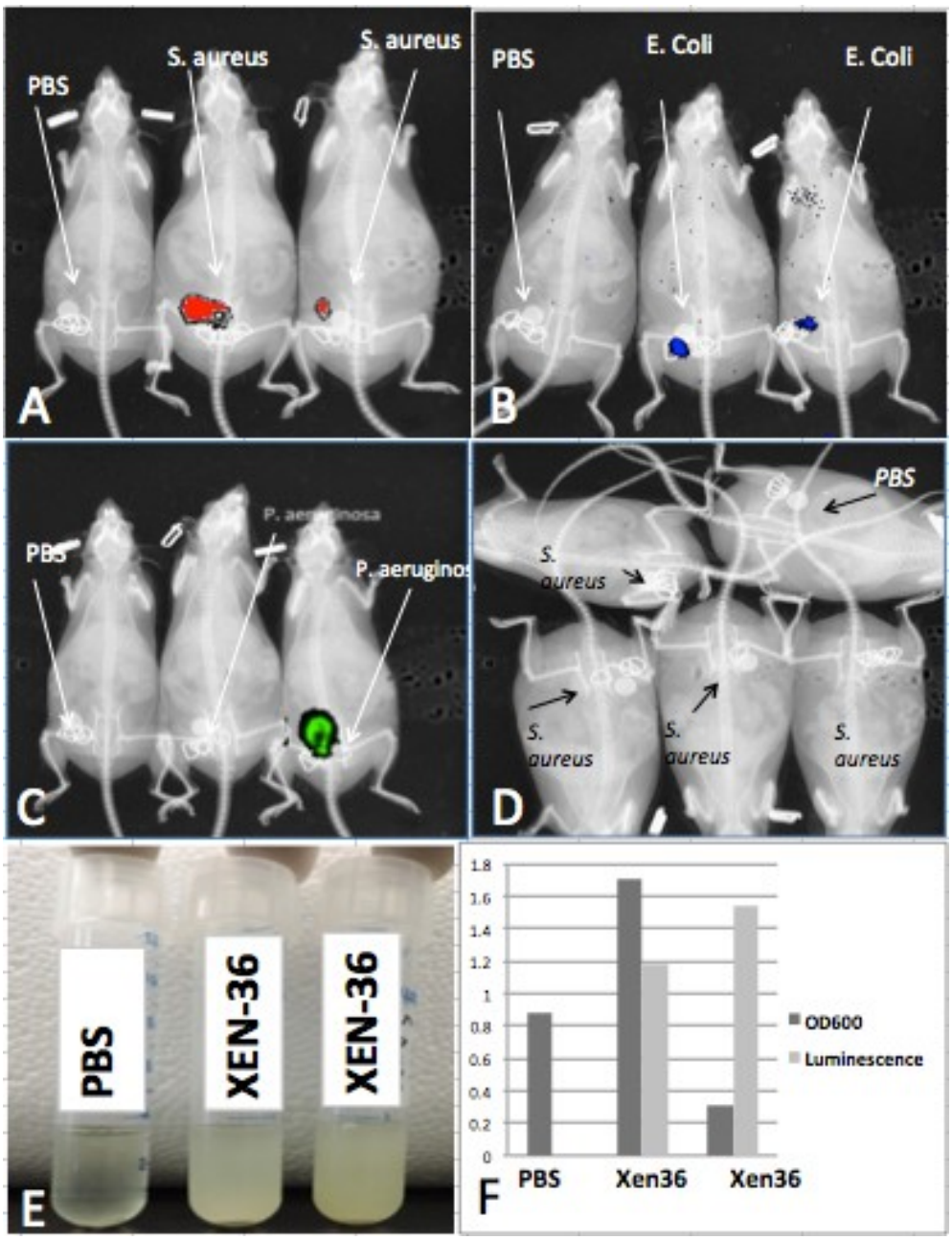

Figure 15. Detection of luminescent bacteria *in vivo*. Pilot studies were performed in order to determine the ideal infectious time frame for determining efficacy of the coated discs *in vivo*. Mice were subcutaneously implanted with uncoated titanium discs and injected with PBS, *S. aureus* (Xen-36), *E. coli* (Xen-16), or *P. aeruginosa* (Xen-5), as indicated. Mice were imaged using an MS/FX-Pro at 2 weeks (D) or 4 days (A, B, C) post-surgery. Mice were euthanized, and discs were retrieved and cultured in 5 mL LB overnight at 37°C. Representative culture samples from *S. aureus* (Xen-36) injected mice from panel A are shown (E); (F) graphical representation of OD_{600} and luminescent measurements of samples from panel E.

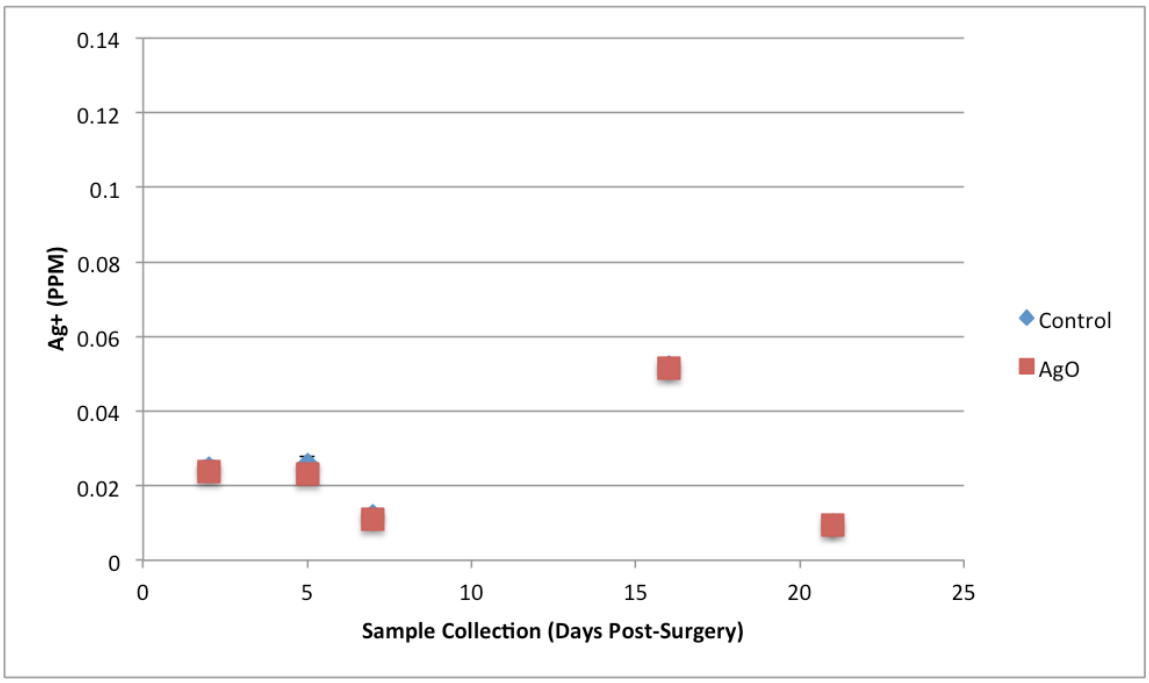

Figure 16. Blood analysis of mice subcutaneously implanted with Ag_xO-coated discs. Five mice were subcutaneously implanted with titanium control discs or double-sided 150 nm Ag_xO-coated discs. Blood samples were obtained at various days following surgery and analyzed by ICP-MS to determine serum silver concentration.

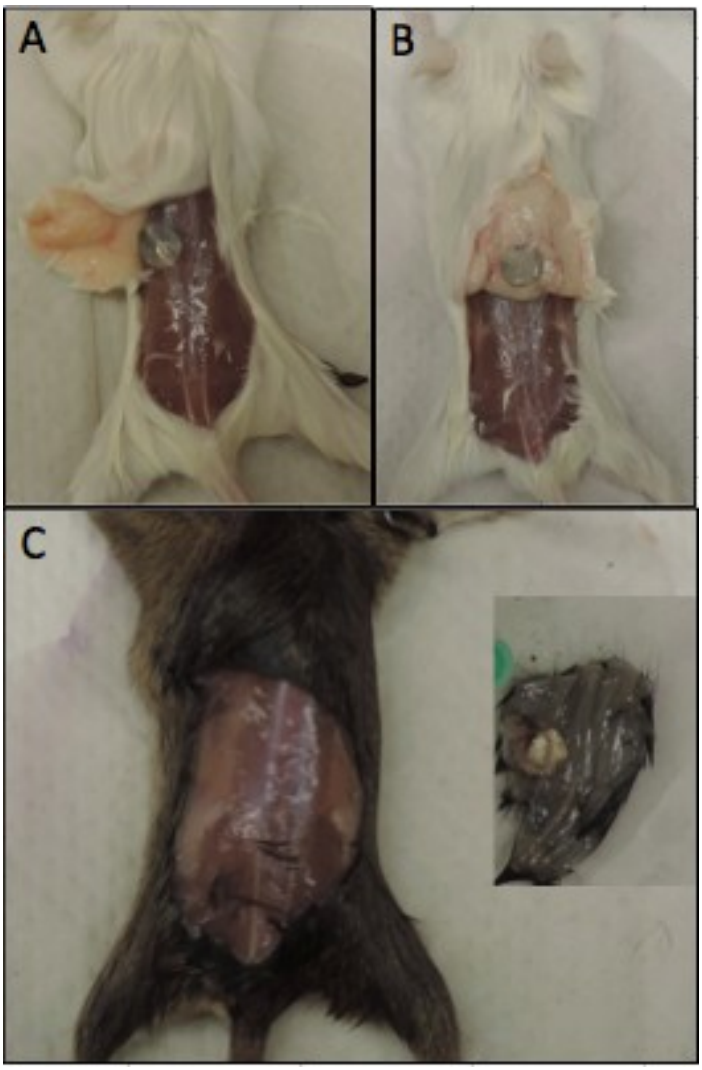

Figure 17. Ag_xO coated discs do not appear to cause damage to cutaneous tissue. Approximately six weeks post-surgery, mice implanted with AgxO coated discs showed no obvious signs of cutaneous tissue damage (B & C) compared to uncoated control discs (A). Inset (C) shows a closer view of the discs on the tissue.

Chapter 4

Extension of Silver Oxide Coatings to Materials for Biomedical Applications

Introduction

When dealing with coatings for medical devices or other medical settings, an important aspect of development is the ability to control the elution rate of an active component from the surface. This is applicable to coatings that are designed to elute an active component, as well as those coatings that are intended to remain static on the surface. Many factors influence the desired elution rate: surface substrate, intended bacterial targets, type of implant, and coating composition. It has thus far been observed that Ag_xO is a viable candidate for coating surfaces and/or implants to provide antimicrobial functionality. In an attempt to further control the elution rate of Ag^+, formulations can be manipulated to contain additional components to modulate Ag^+ elution. By using mixed compositions to create new antimicrobial coatings, the activity, toxicity, biocompatibility, and cost of manufacturing will be affected.

In addition to being a favorable candidate for implant coatings, silver could also be considered for other aspects of healthcare as a partial or full antibiotic replacement. One such viable example is that of a liquid bandage, yet the delivery solvent, dependent on the specific application, could vary. Currently, liquid bandages are commonly made of octyl-2-cyanoacrylate, a longer-chain cyanoacrylate approved by the FDA specifically for this purpose, although many researchers have tried to alter the structure to provide more flexibility[121]. A variety of biomaterials are candidates for such applications, due to their biodegradability and biocompatibility with host extracellular matrix, which gives them the distinct ability to be recognized and accepted by the human body[122-123]. These

biodegradability and biocompatibility properties, along with the variety of naturally derived biomaterials, provide a viable and diverse set of scaffolds as substrates for drug delivery.

Silks are an example of biomaterials that are used widely in textile manufacturing due to their strength[124]. The silk fibroin proteins in particular exhibit greater durability compared to many other biomaterials, providing the possibility of longer-term applications[47]. The durability of silk-based materials can be manipulated, adding a level of tunability for specific applications. Silk fibroin proteins are derived from *Bombyx mori* silkworms, and adopt a functional hetero-dimeric beta-sheet structure. The hetero-dimer consists of two proteins, a heavy chain (~370 kDa), and a light chain (~26 kDa), which are covalently connected through a disulfide bond. The anti-parallel beta-sheet structure in the hetero-dimer is formed primarily from 12 repeating hydrophobic motifs[124-129] (Figure 18). The strength and materials properties of silk proteins have been extensively studied, and were found to be as strong as, or in some tests stronger than, synthetic high-performance polymer fibers[125-129]. In addition, the silk fiber is coated by a secondary protein known as sericin, which acts as an adhesive between fibers, but can also be manipulated for material applications[130]. Given the compositional flexibility, durability, and biodegradability of silk fibroin polymers, they can likely be combined with other proteins, such as elastin, to form complexes suitable for biomedical purposes.

Bandages are a ubiquitous example of a simple medical device used to ameliorate the effects of abrasions and lacerations in both hospital and home settings to help prevent infection. Often, commercially available bandages are supplemented with topical antibiotics as bacitracin zinc, neomycin sulfate, polymyxin B, or some combination of

these, yet recent studies have shown that these antibiotic-loaded bandages are not as effective at reducing bacterial loads in wounds as previously believed[131-132]. Continued use of these antibiotic-impregnated bandages will likely contribute to increased resistance development, and hence render them less effective over time. Silver-coated bandages have often been applied in the treatment of burn wounds[27, 133-134] yet recently, these silver-coated bandages have been considered as an alternative to traditional antibiotic bandage coatings in the treatment of standard abrasions and incision wounds[135-136]. As such, the antimicrobial efficacy of these bandages will be directly linked to the elution rate of Ag^+ or Ag-containing compounds from the bandages to the wound site.

As mentioned previously, the antimicrobial properties of metals such as mercury, arsenic, silver, and copper have been known for years, but were often overlooked with the dawn of the age of small molecule antibiotics[137]. Of these metals, silver is currently the most widespread in antimicrobial applications, yet copper has also garnered significant interest for antimicrobial properties. Metallic copper surfaces have been widely examined for their contact killing abilities, which were proven effective against a variety of bacterial species[138]. When investigated as a coating for surfaces, copper and copper alloys showed significant bacterial inhibition against both *E. coli* and MRSA at various bacterial loads[139]. However, like silver, copper has limited solubility in aqueous environments, thus limiting the ability to elute active Cu^+/Cu^{2+} into a wound site. Mixtures of CuO and Ag_xO present the potential advantage of modulating release rate of Ag^+ ions into solution, because CuO is effectively insoluble in water. This would allow facile synthesis of mixed Ag_xO/CuO layers, in which the relative ratios of the components are varied to tune elution properties. Noting the elution profiles of

substances used is important to maintain the antimicrobial activity of the coatings themselves, as well as eliminate any potential toxicity induced by elution that occurs too quickly[140-141].

The goal of the following studies was to utilize Ag_xO in similar ways to those previously tested in an attempt to widen the potential market for Ag_xO coating technology, as well as further understand and utilize the ability to alter the elution profiles of formed coatings. To do this, coatings were embedded in silk fibroin proteins, applied to standard bandages, and combined with CuO to test and compare efficacy to standard Ag_xO coatings in similar assays as those completed in previous chapters.

Materials and Methods

Generation of silk films and silk film deposition. To extract silk proteins, raw cocoons were cut and washed, rinsed with sodium carbonate, and boiled, as reported previously[124]. Extracted fibers are rinsed multiple times and dried in an oven. The dried fibers are dissolved in LiBr solution and subjected to dialysis against water to further separate the silk fiber proteins. The sample is then centrifuged, and concentration determined by dry weight analysis[128].

To create impregnated films, the desired amount of solid AgO or Rhodamine 6G was added to silk solution and dissolved by mixing. Aliquots of these solutions were added to individual wells of 96-well plates and were dried using ambient airflow in a chemical fume hood overnight. The following day, films were twice rinsed with methanol to solidify the film and prevent flaking during experimentation. The creation of multi-layered films followed the same procedure in sequence.

Rhodamine release assay. A specified amount of PBS was added to each of the test wells containing silk films, regardless of composition, and the plate was placed in the incubator at 37°C for 1 hour. Following incubation, a portion of the PBS solution in each well was transferred to a fresh 96-well plate for fluorescence reading.

Bacterial culturing. Protocol followed is explained in Chapter 2, Materials and Methods section labeled 'Bacterial culturing'.

Modified minimum inhibitory concentration (mMIC). The modified version of the broth micro-dilution assay was used to determine the antimicrobial activity of the silver impregnated silk films. This is modified, as silver is not added in solution, but it is present in a solid film at the bottom of the well, thus restricting the soluble silver in the wells. The modified MIC plates were prepared with AgO-impregnated silk containing varying concentrations of AgO in the films (ranging from 0%-0.5% by weight). To each coated well, 200µL of bacterial culture ($0.5x10^5$ CFU/mL), or blank LB broth was added, providing test replicates as well as controls for each concentration of AgO film. Plates were covered and placed in the incubator at 37°C overnight. Following incubation, plates were removed from the incubator and photographed before 100µL was transferred from each well into a fresh 96 well plate. Absorbance measurements were performed on these 100µL aliquots at 600nm using a Molecular Devices Spectramax M5. An additional aliquot of 50µL was removed from selected wells from the original plate and spread onto LB agar plates. These LB agar plates were incubated at 37°C overnight and colonies were counted following incubation to assess growth and investigate bactericidal vs. bacteriostatic activity.

Bacterial growth curve analysis. Protocol followed is explained in Chapter 2, Materials and Methods section labeled 'Bacterial culturing'.

ZOI. Protocol followed is explained in Chapter 2, Materials and Methods section labeled 'Bacterial culturing'.

Results

Silk biopolymers as an antibacterial delivery platform. In order to examine the ability of silk films to deliver silver oxide to kill bacteria, a fluorescent reporter, Rhodamine 6G, was used to assay release from silk biopolymer films deposited in 96-well plates. The films were constructed in a dual-layer format such that only one of the two layers (top, bottom) contained the Rhodamine. This experiment was designed to determine whether the Rhodamine release was affected by the exposure to the aqueous environment and/or the presence of an additional blocking layer of silk biopolymer. Results of this experiment, shown in Figure 19, show that there was greater release of Rhodamine into the aqueous milieu when the Rhodamine-containing layer was the top layer of the film. When the Rhodamine-containing layer was concealed by an undoped silk biopolymer layer, release still occurred, but to a lesser extent.

Previous work has demonstrated that silver oxide is an effective antimicrobial agent when applied as a surface coating to titanium; this coating component has been extended to several alternative delivery methods. Figure 20 shows a sample 96-well plate containing AgO-impregnated silk films at varying AgO concentrations. This image shows that the films are relatively homogeneous at the macroscopic level with coloration changes as AgO concentrations increase. A modified MIC (mMIC) for these types of

films was determined by incubating the films with bacterial cultures of either *S. aureus* (Figure 21) or *E. coli* (data not shown). The mMIC for *S. aureus* was found to be somewhat variable, ranging between 0.1% - 0.25% AgO. The results for *E. coli*, however, are confounded by inherent antimicrobial activity from the silk, either from the biopolymer itself or remnants of the purification process.

In addition to determining mMICs for AgO-impregnated silk films, films impregnated with silver nanoparticles or films coated with AgO via reactive sputtering were also examined. Figure 22 shows the results of the zone of inhibition assay using silk films with each of the previously described compositions. Universally, consistent with the mMIC findings, the measured ZOI for all compositions was larger against *E. coli* than *S. aureus*. However, in both cases, the sputter-coated AgO performed similarly to impregnated silver nanoparticles, both of which performed slightly better than AgO-impregnated films.

A comparison of these materials was also performed as a bacterial growth curve analysis, as described above. The results show that all three silver/silk material forms inhibited bacterial growth for both *S. aureus* and *E. coli* (Figure 23). As presented previously, in this experimental environment, *E. coli* was showed greater inhibition compared to *S. aureus* in both experimental duplicates as well as across impregnated AgO, silver nanoparticles, and Ag_xO sputtered silk. In the cases of both the *S. aureus* and *E. coli*, growth inhibition occurred with all silver-containing discs, although the Gram-positive *S. aureus* experienced the most antibacterial activity from the silver-sputtered silk discs.

Application of coatings formed by reactive sputtering applied to bandages. In an effort to assess the antimicrobial properties of silver-sputtered bandages as compared to standard, commercially available bandages (both antibiotic-coated and regular, uncoated) zone of inhibition assays were performed with varying bacterial species (Figure 24). In the cases of both the *S. aureus* and *E. coli*, uncoated bandages showed no inhibition to bacterial growth on the surface, while the antibiotic-coated bandages showed little to no growth. Although growth on the *E. coli* plate was less dense than *S. aureus*, a zone of inhibition of decent size was present on each plate. In addition to surface bacterial testing, solution kinetics testing was also performed to test the efficiency of elution over a length of time (Figure 25). In the case of each bacterial species tested, the test tubes containing AgO-coated bandages showed no increase in growth throughout the length of the experiment, while the control, standard bandages, and antibiotic-coated bandages all showed rapid growth increases. In all cases, there was little to no difference between the control, regular, and antibiotic-coatings.

Evaluation of Ag_xO/CuO films as next-generation antimicrobial coatings. A series of Ag_xO/CuO coatings in which the Ag_xO/CuO ratio was varied (Table 2), deposited on high-density polyethylene (HDPE). These different film compositions were tested for antimicrobial activity be performing zone of inhibition assays (Figure 26). All compositions tested induced a zone of inhibition against *S. aureus* and *E. coli*, with the exception of composition #71 (10 Ag, 70 Cu). These coatings were also tested in growth curve experiments (Figure 27). In these experiments, the most effective compositions at inhibiting bacterial growth were the mixtures that contained Ag_xO as the major component. Composition #71 was ineffective against both bacterial species tested, and

composition #73 was more effective against *S. aureus* than *E. coli*, yet not as effective as samples with higher silver oxide concentration.

Discussion

Overall, the experimental results presented show an inhibition of growth in culture and on surfaces with various application methods of AgO (impregnated or sputtered, etc.) as well as Ag_xO/CuO mixtures. The flexibility of surfaces on which Ag_xO coatings and coating mixtures can be applied allows for a great number of future possible applications.

Biomaterials provide a natural and biodegradable platform to deliver silver to surface wounds, preventing bacteria from infecting the wound. Using films composed of Mori silk provided a flexible, biodegradable material to deliver silver and potentially other compounds. While the biopolymer films had exhibited favorable properties for silver delivery, the process involved in creating the films, as well as materials properties changes upon Ag_xO deposition by sputtering, may affect the future range of applications. Specifically, the silk biopolymer films became very brittle after sputtering deposition, which would limit the ways these materials could be molded for final application. In addition, due to the poor solubility of AgO in water[142], attaining a uniform distribution of AgO in impregnated films was more difficult than anticipated (final results shown in Figure 20). Whether or not universal distribution of AgO solid could occur in a different concentration of silk solution was not investigated. While this non-uniform distribution did not appear to affect the activity in our experiments, it may present challenges and variability in behavior when scaled up. In the experiments performed, however, this

heterogeneous distribution was likely a result of the properties of silver oxide, as our experiments with Rhodamine resulted in a more uniform coating and differential release based on the multilayer structure (Figure 19). Rhodamine release was observed in both cases, but the films that contained Rhodamine in the top layer, exhibited higher fluorescence than those in which Rhodamine was embedded in the bottom layer. This indicates that Rhodamine release from the lower layer was obstructed by the presence of the second layer of silk, as expected. Using this methodology, we propose it would be possible to deliver different amounts of AgO and control the rate of release, providing a longer-lasting antimicrobial effect. Additionally, the experiments performed were a single time point analysis, so determining the kinetics of release in these systems is also of interest for future experiments.

The minimum inhibitory concentrations were determined for both *S. aureus* (Figure 21) and *E. coli* using AgO-embedded silks deposited on the surface of a 96-well plate. The value for *S. aureus* proved to be more difficult to determine than *E. coli*. This is consistent with previous observations in which higher concentrations of AgO were required for activity against *S. aureus* compared to *E. coli*. The heterogeneity in the AgO-impregnated silk films may result in batch-to-batch differences, resulting in differential release of AgO into the wells, and thus potentially delivering below the concentration required for activity in some replicates. Testing on bacteria-loaded surfaces (Figure 22) and in solution (Figure 23) proved that in the majority of cases, AgO-impregnated silk films provided equal efficacy as 0.1% silver nanoparticles, and 150nm AgO sputtered silk films. In both solid and liquid culture, *S. aureus* proved more difficult to inhibit (Figure 22B, Figure 23B), consistent with our other findings. This held true for the silver

nanoparticles as well as the Ag_xO-sputtered pieces, however the silk impregnated pieces showed greater growth reduction than all other test pieces.

The use of bandages is ubiquitous in the treatment of lesions, abrasions, and other wound types. The ability of bandages to aid in wound healing is important in the prevention of infection by providing a barrier between the open wound and the environment. Many bandages also contain one of more standard small molecule antibiotics to aid in infection control, however they are becoming increasingly unable to fulfill this task, a new alternative is imperative[131]. Silver-coated bandages were examined for antimicrobial efficacy on solid media (Figure 24) and in solution (Figure 25) and compared to traditional, commercially available antibiotic-loaded bandages, as well as standard bandages. Although the size of the bandages used in ZOI tests were somewhat variable, it is evident from the data that the AgO-coated bandages were far superior in inhibiting growth of *S. aureus*, shown in Figure 24A. The commercially available antibiotic bandages were completely ineffective at inhibiting *S. aureus* growth, providing a dramatic proof of concept in the potential efficacy of these coatings for bandage applications. This trend can also be seen for *E. coli* in Figure 24B, although the initial results are inconclusive due to the incomplete growth of a bacterial lawn on the plates. The solution growth kinetics performed yielded similar results, as the AgO-sputtered bandages showed a greater growth inhibition than the standard uncoated bandages or commercially available antibiotic coated bandages. Further testing is necessary to determine a sufficient the dose needed to inhibit bacterial growth at the wound site, as well as the effects of those dosages to the immediate wound area, surrounding skin, and overall wound healing process.

While exploring alternative ways to control the elution rate from AgO coatings, mixing AgO with other known antimicrobials was proposed. AgO/CuO mixtures were sputtered onto plastic substrates and tested as an alternative coating material. The rationale was that the CuO is practically insoluble in water, and thereby could provide a means of modulating the release of Ag^+ from AgO-containing surfaces. ZOI testing was performed on each of the six mixtures prepared, using both *E. coli* (Figure 26A) and *S. aureus* (Figure 26B). All mixtures showed similar efficacy in producing a ZOI, except for #71, the composition containing the least AgO in the mixture. Solution testing was performed on each of the mixtures as well, against both *E. coli* (Figures 287A and 27B) and *S. aureus* (Figures 27C and 27D). In these experiments, *E. coli* growth was inhibited by each of the mixtures, while *S. aureus* only showed complete inhibition with mixtures containing at least 30 Ag. From these results, it can be deduced that the AgO portion of the mixtures provided the majority of antimicrobial activity in these cases, and CuO appears to serve as a viable method to control the elution rate of Ag^+. Future experiments will focus on quantifying the release rates of Ag into solution from different AgO/CuO mixtures, as well as determining the ability of the AgO/CuO films to prevent adhesion to surfaces before and after all Ag^+ is released into solution.

Conclusion

In these studies, various delivery methods of AgO were examined, as well as CuO as an additive to AgO sputtered coatings as a way to control the elution rate of coatings from the surface. Silk biofilms were used as a delivery method for impregnated AgO solid, with future application to surface punctures and wounds as an alternative to traditional bandages. In addition, AgO-coated bandages exhibited a greater antimicrobial

effect than that of the standard, commercially available antibiotic coated bandages, indicating that they may become a viable alternative to standard bandages. Finally, adding CuO to previously tested AgO formulations did not significantly effect the ability to inhibit bacterial growth, however growth inhibition was dependent on AgO:CuO ratio in the films. This is thought to be a result of CuO modulating the release rate of the AgO. Finally, using AgO/CuO mixtures would make the technology more affordable, as Cu is a less expensive material than Ag. In total, these varied applications and materials demonstrate the flexibility of AgO coatings produced by reactive sputtering for a variety of biomedical applications.

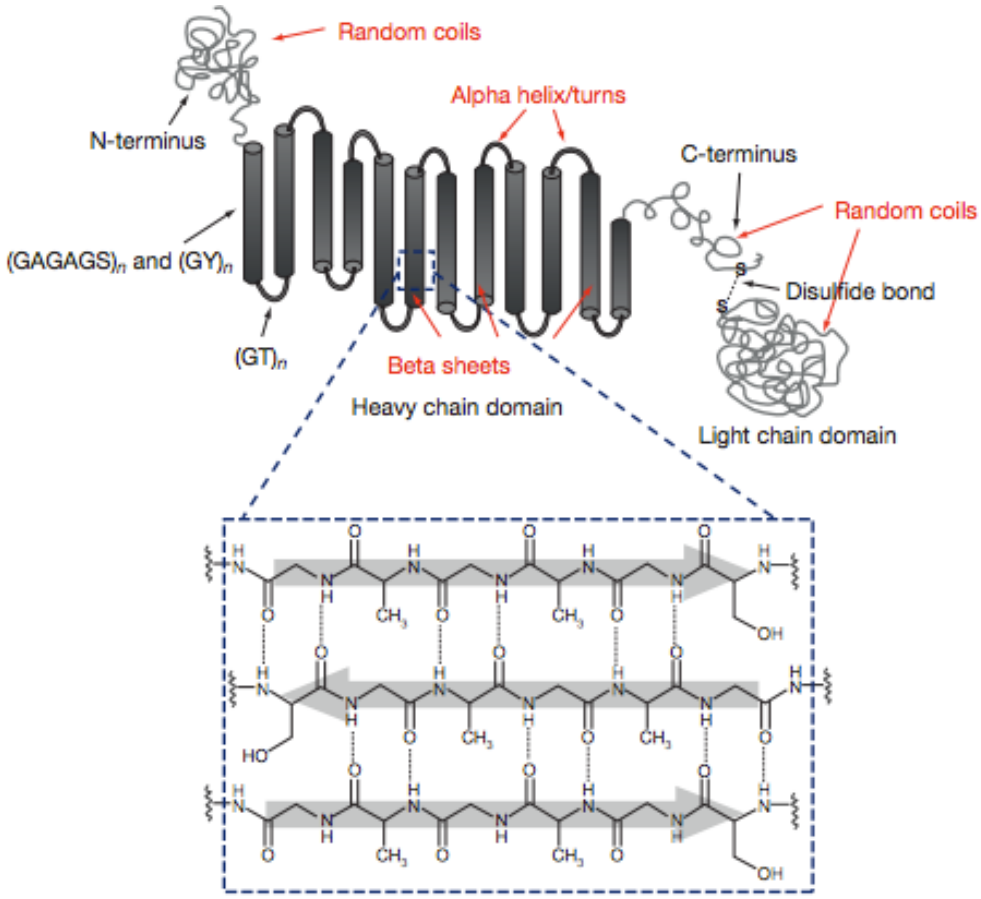

Figure 18. Secondary structure of one *B. mori* silk fibroin chain; (Gly-Ala-Gly-Ala-Gly-Ser) amino acid repeat units that self-assemble into antiparallel beta sheets. Figure modified[143-144].

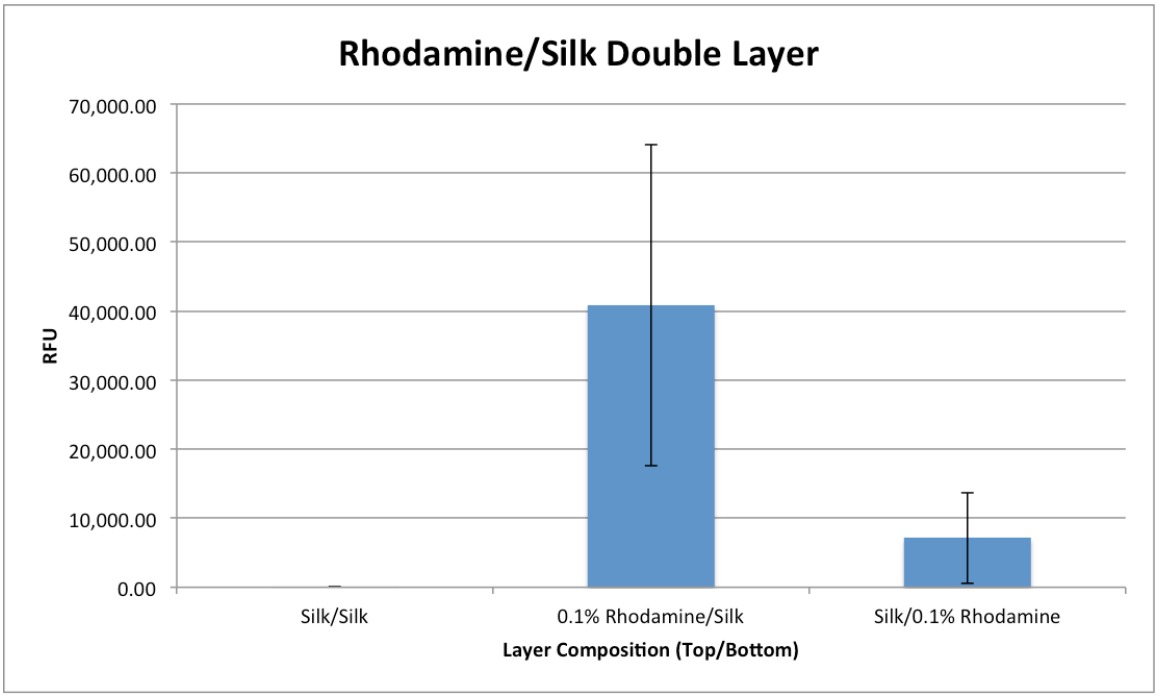

Figure 19. Rhodamine release comparison form multi-layered silk films. Rhodamine fluorescence from the supernatant collected after exposure to multi-layered silk films. Fluorescence measurements were taken of films composed of two layers of pure silk, a layer of Rhodamine-impregnated silk on top of a layer of pure silk, and a layer of pure silk over a layer of Rhodamine-impregnated silk. n=16.

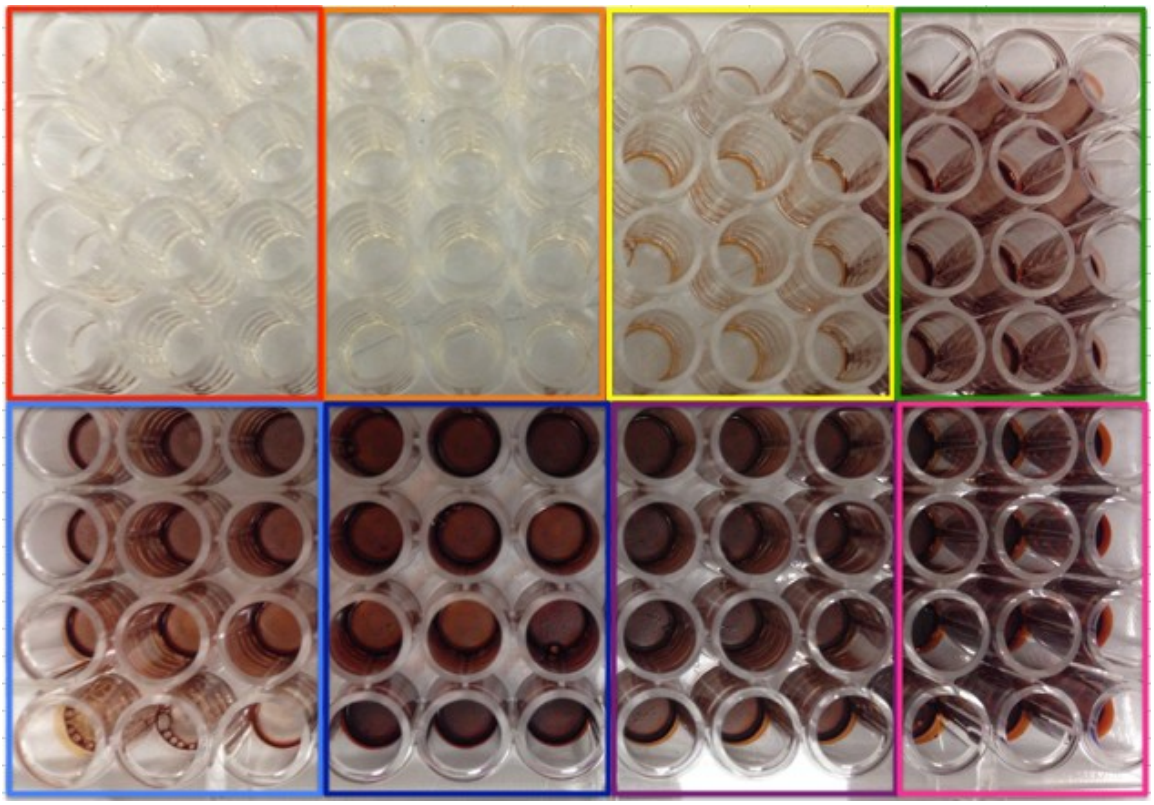

Figure 20. Silk films deposited on the bottom of 96 well plate. Various concentrations of silk/silver were deposited on the bottom of individual wells of a 96 well plate. Concentrations are outlined in to highlight variations in silver concentration. Red – 0% AgO, orange – 0.001% AgO, yellow – 0.005% AgO, green – 0.01% AgO, light blue – 0.1% AgO, dark blue – 0.25% AgO, purple – 0.35% AgO, pink – 0.5% AgO.

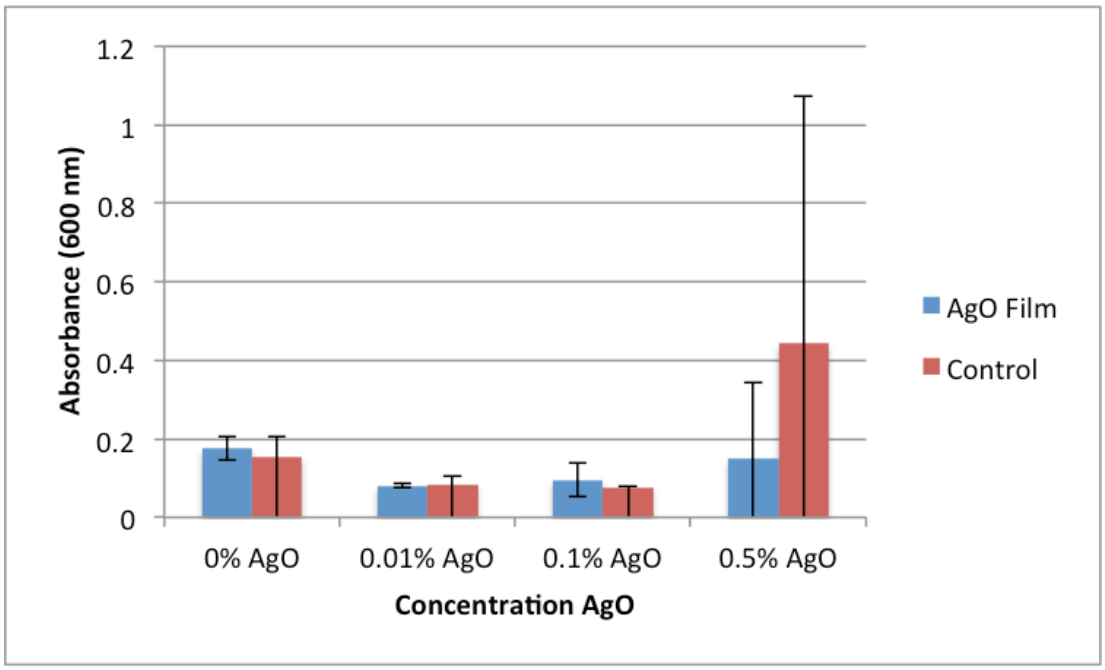

Figure 21. Modified minimum inhibitory concentrations for *S. aureus*. All MIC concentrations were confirmed 2-4 times in varying replicates, and replicates are shown as means with standard deviation over all wells tested containing films with the same concentration of impregnated AgO.

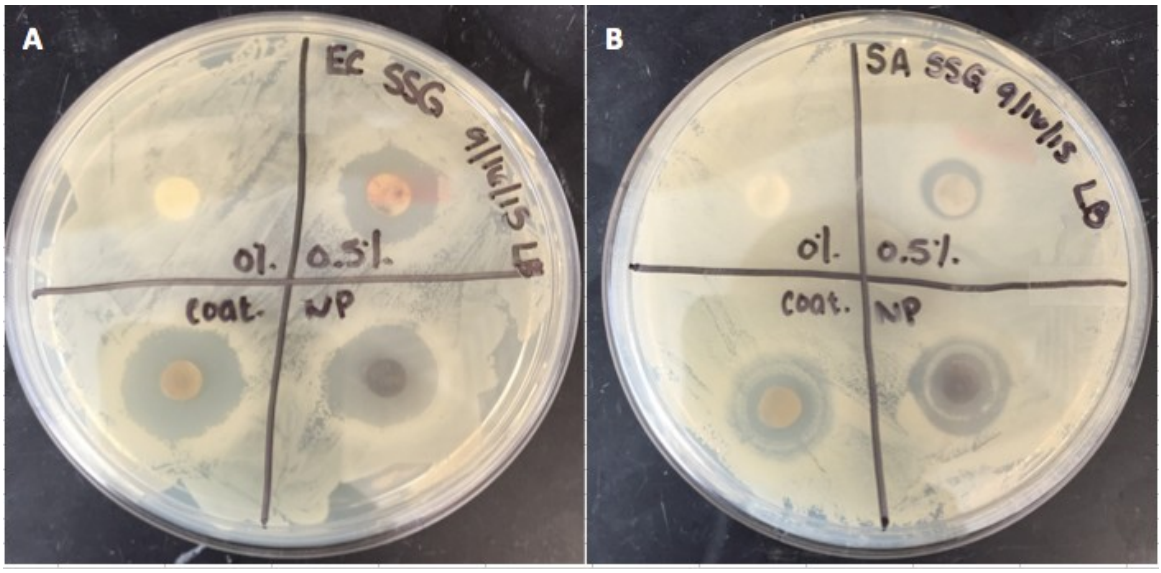

Figure 22. Zone of inhibition analysis for various silk films containing silver. Zone of inhibition for (a) *E. coli* and (b) *S. aureus.* Test discs containing 0% AgO (pure silk control), 0.5% AgO (impregnated), 0.1% silver nanoparticles (impregnated), or 150nm Ag_xO sputtered surface coating. Zone of inhibition measured for *E. coli*: exhibited a 1.6 cm zone for 0.5% AgO, 1.8 cm zone for 0.1% silver nanoparticles, 1.9 cm zone for the Ag_xO sputtered surface, and no zone for the 0% AgO control. Zone of inhibition measured for *S. aureus*: 1 cm zone for 0.5% AgO, 1.5 cm outer zone for 0.1% silver nanoparticles, 1.6 cm outer zone for the Ag_xO sputtered surface, and no zone for 0% AgO control. All test discs are 0.635 cm diameter. Plates were seeded with a known concentration of bacteria, discs were applied to the surface and the plates were grown at 37°C overnight before measurement and imaging.

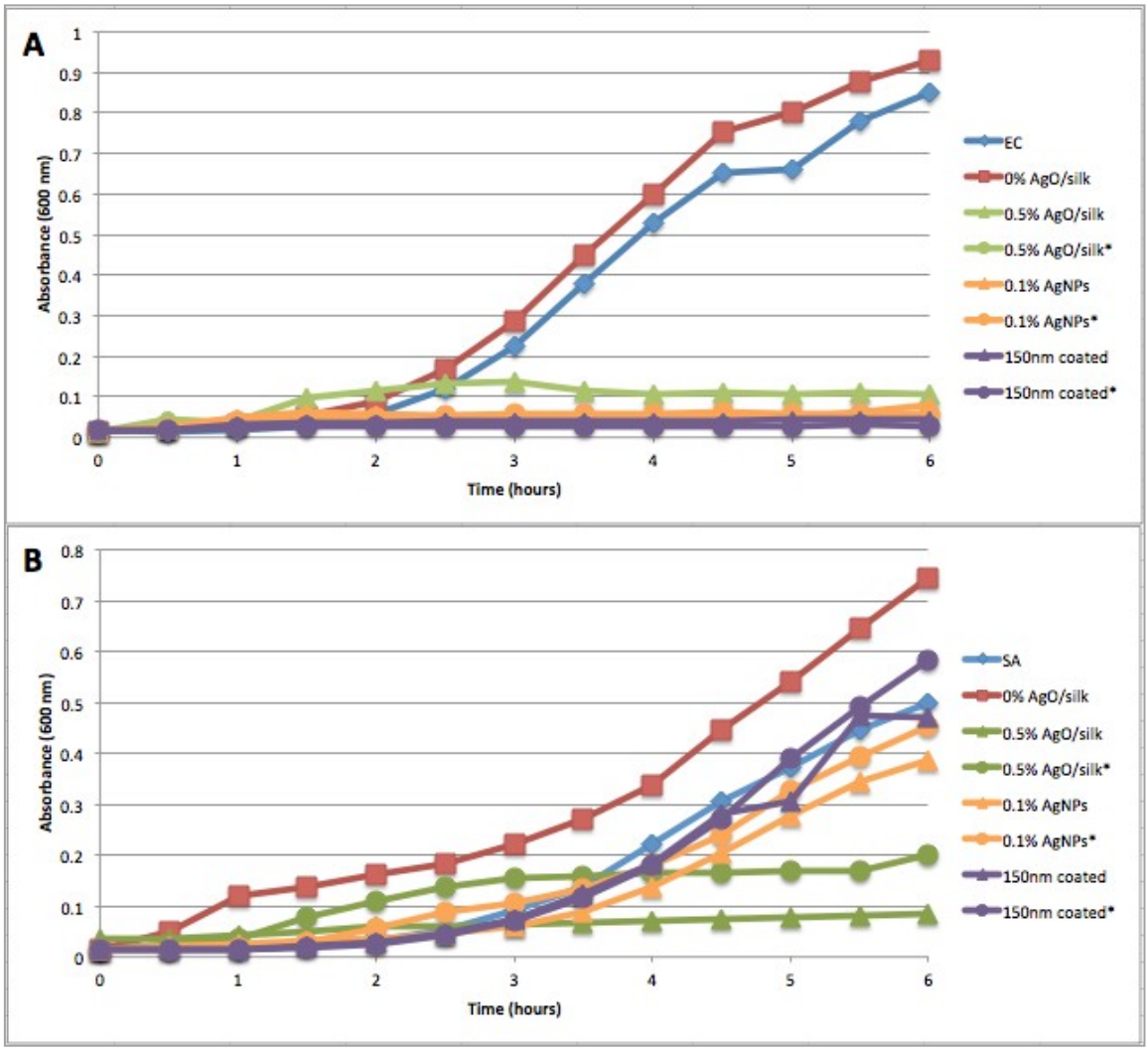

Figure 23. Growth curve analysis in solution. Silk film discs containing either 0% AgO, 0.5% AgO (green), 0.1% silver nanoparticles (orange), or Ag_xO 150nm sputtered (purple) discs were placed into (a) *E. coli* (starting concentration of $1.25x10^6$ CFU/mL), (b) *S. aureus* (starting concentration of $1.17x10^5$ CFU/mL). Data are color coded according to replicates.

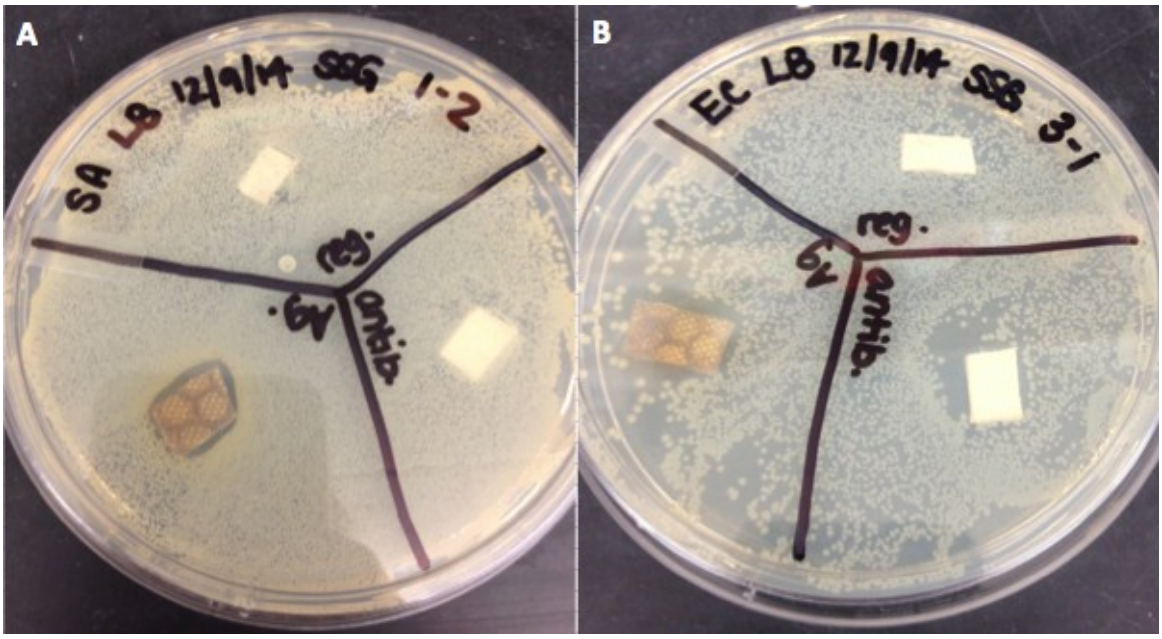

Figure 24. Zone of inhibition testing for various bandage types. Zone of inhibition for (a) *S. aureus* and (b) *E. coli.* Standard, commercially-available uncoated bandages, antibiotic coated (Polymyxin B Sulfate 10,000 units and Bacitracin Zinc 500 units per gram), and Ag_xO sputtered bandages were tested. Plates were seeded with a known concentration of bacteria, bandages were applied to the surface and the plates were grown at 37°C overnight before imaging.

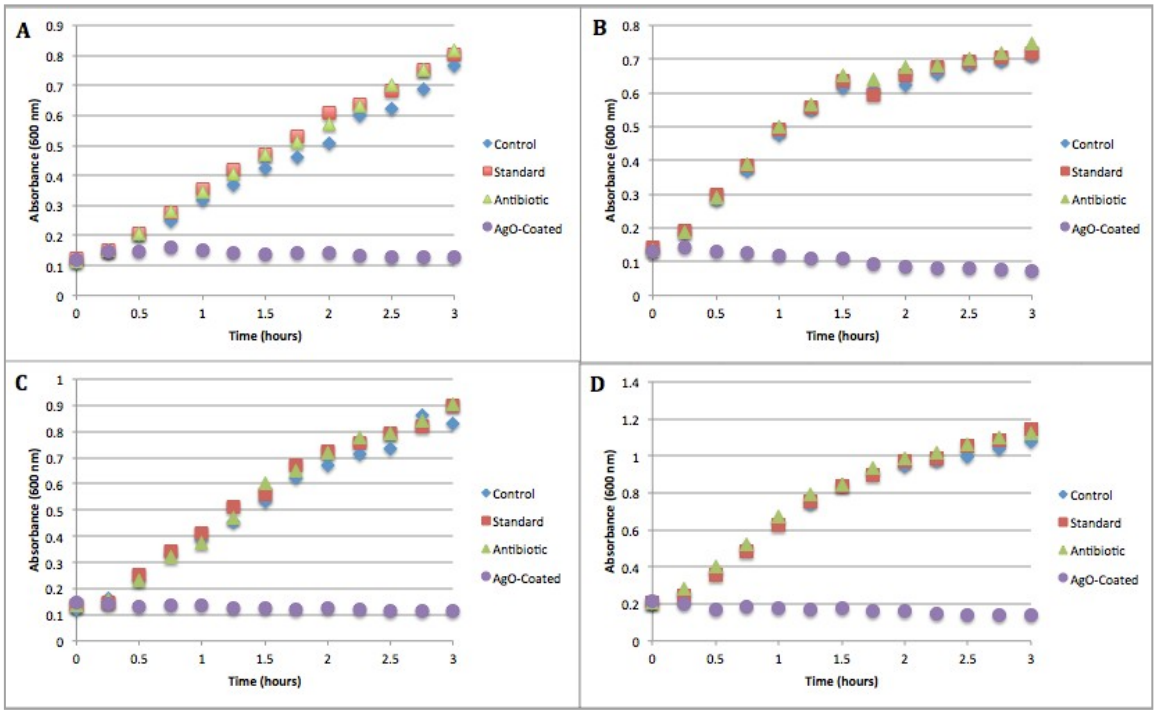

Figure 25. Growth curve analysis of bandages in solution. Standard uncoated, antibiotic-impregnated (Polymyxin B Sulfate 10,000 units and Bacitracin Zinc 500 units per gram), and AgxO sputtered bandages were tested for antimicrobial efficacy in solution. Strains examined were: (a) S. aureus (starting concentration 1.13×10^7 CFU/mL), (b) *E. coli* (starting concentration 1.51×10^8 CFU/mL), (c) *P. aeruginosa* (starting concentration 1.06×10^8 CFU/mL), and (d) *K. pneumoniae* (starting concentration 1.49×10^7 CFU/mL). All test bandages were cut to approximately the same dimensions to minimize potential differences in dosing.

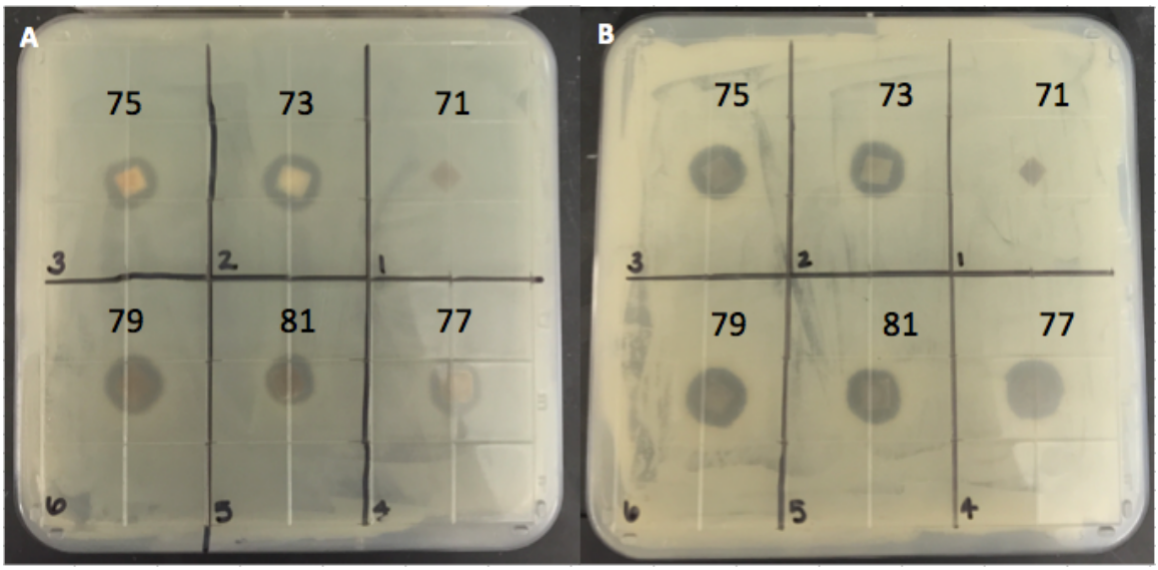

Figure 26. Zone of inhibition testing for silver oxide/copper mixtures. Zone of inhibition for (a) *E. coli* and (b) *S. aureus*. (A) exhibited no zone at 71, 1 cm zone at 73, 0.9 cm zone at 75, 1 cm zone at 77, 1 cm zone at 81, and 0.8 cm zone at 79. (B) exhibited no zone at 1, 1 cm zone at 73, 0.9 cm zone at 75, 1 cm zone at 77, 1 cm zone at 81, and 0.9 cm zone at 79. Concentrations for each composition are listed in Table 2.

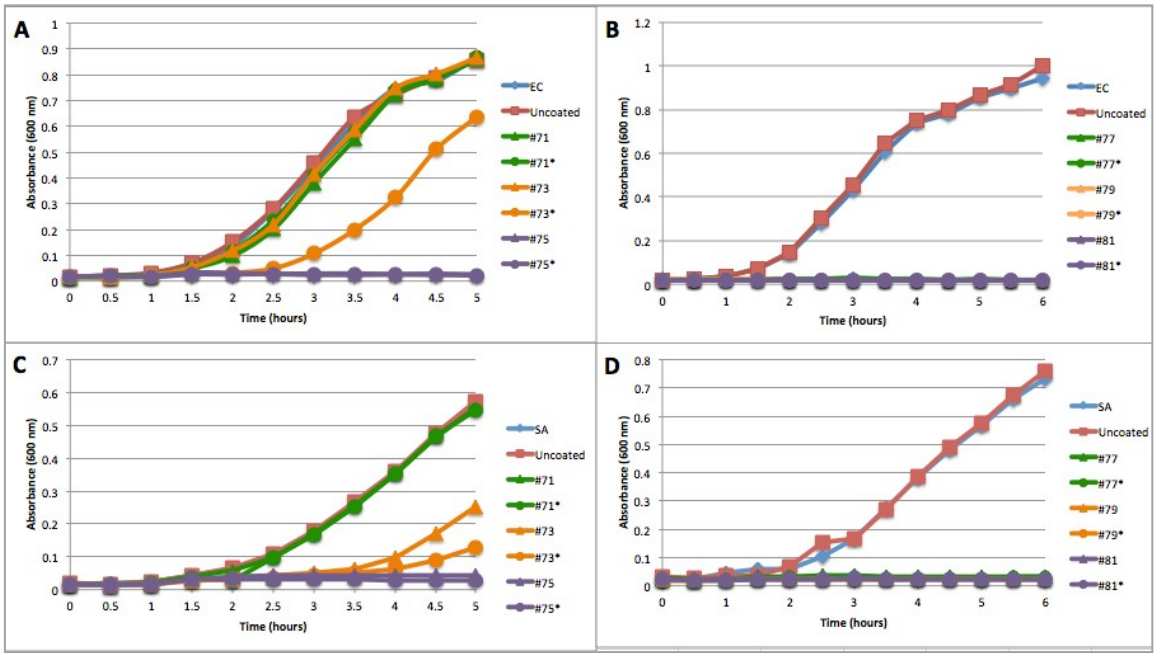

Figure 27. Growth curve analysis of copper oxide/silver oxide mixtures. Coatings were deposited on high-density polyethylene (HDPE). Uncoated pieces were used as the control. Pieces were tested against (a, b) *E. coli* (starting concentrations 1.47×10^6 CFU/mL and 1.81×10^6 CFU/mL, respectively) and (c, d) *S. aureus* (starting concentrations 1.24×10^5 CFU/mL and 1.47×10^5 CFU/mL, respectively). All test pieces were squares approximately sized 3/16" per side. Coating composition varied from sample to sample, and is described in Table 2. The numbers in the legend correspond to the sample numbers in Table 2.

Table 2.

Ag_xO/CuO Coating Compositions.

Sample Number	Composition
71	10 Ag, 70 Cu
73	20 Ag, 60 Cu
75	30 Ag, 60 Cu
77	40 Ag, 50 Cu
79	50 Ag, 40 Cu
81	60 Ag, 30 Cu

References

[1] WHO *Antimicrobial Resistance Global Report*; 2014.

[2] Yoneyama, H.; Katsumata, R., Antibiotic resistance in bacteria and its future for novel antibiotic development. *Biosci Biotechnol Biochem* **2006,** *70* (5), 1060-75.

[3] Abraham, E. P.; Chain, E. B., An enzyme from bacteria able to destroy penicillin. *Nature* **1939,** *146* (3713), 837.

[4] Laxminarayan, R.; Duse, A.; Wattal, C.; Zaidi, A. K.; Wertheim, H. F.; Sumpradit, N.; Vlieghe, E.; Hara, G. L.; Gould, I. M.; Goossens, H.; Greko, C.; So, A. D.; Bigdeli, M.; Tomson, G.; Woodhouse, W.; Ombaka, E.; Peralta, A. Q.; Qamar, F. N.; Mir, F.; Kariuki, S.; Bhutta, Z. A.; Coates, A.; Bergstrom, R.; Wright, G. D.; Brown, E. D.; Cars, O., Antibiotic resistance-the need for global solutions. *Lancet Infect Dis* **2013,** *13* (12), 1057-98.

[5] CDC *Antibiotic resistance threats in the United States, 2013*; US Centers for Disease Control and Prevention: 2013.

[6] Howard, D.; Rask, K., The impact on resistance on antibiotic demand in patients with ear infections. In *Battling resistance to antibiotics and pesticides: an economic approach*, RFF Press: Washington DC, 2002; pp 119-133.

[7] Tran, J. H.; Jacoby, G. A., Mechanism of plasmid-mediated quinolone resistance. *Proc Natl Acad Sci U S A* **2002,** *99* (8), 5638-42.

[8] Meredith, H. R.; Srimani, J. K.; Lee, A. J.; Lopatkin, A. J.; You, L., Collective antibiotic tolerance: mechanisms, dynamics and intervention. *Nat Chem Biol* **2015,** *11* (3), 182-8.

[9] Lentino, J. R., Prosthetic joint infections: bane of orthopedists, challenge for infectious disease specialists. *Clin Infect Dis* **2003,** *36* (9), 1157-61.

[10] Sweidan, M.; Zhang, Y.; Harvey, K.; Yang, Y.; Shen, X.; Yao, K., Proceedings of the 2nd national workshop on rational use of antibiotics in China. *Beijing: Beijing Children's Hospital* **2005**.

[11] Giguère, S., Antimicrobial Drug Action and Interaction. In *Antimicrobial Therapy in Veterinary Medicine, Fifth Edition*, Giguère, S.; Prescott, J. F.; Dowling, P. M., Eds. John Wiley & Sons, Inc.: Hoboken, NJ, 2013.

[12] Woodward, C., Animal antibiotics under tougher United States scrutiny as consensus grows on "superbug" risk to humans. *CMAJ* **2010,** *182* (11), E513-4.

[13] Allen, H. K., Antibiotic resistance gene discovery in food-producing animals. *Curr Opin Microbiol* **2014,** *19*, 25-9.

[14] Jakobsen, L.; Spangholm, D. J.; Pedersen, K.; Jensen, L. B.; Emborg, H. D.; Agerso, Y.; Aarestrup, F. M.; Hammerum, A. M.; Frimodt-Moller, N., Broiler chickens, broiler chicken meat, pigs and pork as sources of ExPEC related virulence genes and resistance in Escherichia coli isolates from community-dwelling humans and UTI patients. *Int J Food Microbiol* **2010,** *142* (1-2), 264-72.

[15] Marshall, B. M.; Levy, S. B., Food animals and antimicrobials: impacts on human health. *Clin Microbiol Rev* **2011,** *24* (4), 718-33.

[16] Sorensen, T. L.; Blom, M.; Monnet, D. L.; Frimodt-Moller, N.; Poulsen, R. L.; Espersen, F., Transient intestinal carriage after ingestion of antibiotic-resistant Enterococcus faecium from chicken and pork. *N Engl J Med* **2001,** *345* (16), 1161-6.

[17] Kuehn, B. M., Some progress in effort to reduce hospital-acquired infections. *JAMA* **2014,** *311* (15), 1488.

[18] CDC *National and State Healthcare Associated Infections*; United States Centers for Disease Control and Prevention: 2016.

[19] Berbari, E. F.; Hanssen, A. D.; Duffy, M. C.; Steckelberg, J. M.; Ilstrup, D. M.; Harmsen, W. S.; Osmon, D. R., Risk factors for prosthetic joint infection: case-control study. *Clin Infect Dis* **1998,** *27* (5), 1247-54.

[20] Petty, W.; Spanier, S.; Shuster, J. J.; Silverthorne, C., The influence of skeletal implants on incidence of infection. Experiments in a canine model. *J Bone Joint Surg Am* **1985,** *67* (8), 1236-44.

[21] Harris, L. G.; Richards, R. G., Staphylococci and implant surfaces: a review. *Injury* **2006,** *37 Suppl 2*, S3-14.

[22] Mah, T. F.; Pitts, B.; Pellock, B.; Walker, G. C.; Stewart, P. S.; O'Toole, G. A., A genetic basis for Pseudomonas aeruginosa biofilm antibiotic resistance. *Nature* **2003,** *426* (6964), 306-10.

[23] Hoyle, B. D.; Costerton, J. W., Bacterial resistance to antibiotics: the role of biofilms. *Prog Drug Res* **1991,** *37*, 91-105.

[24] Wolcott, R. D.; Rhoads, D. D.; Bennett, M. E.; Wolcott, B. M.; Gogokhia, L.; Costerton, J. W.; Dowd, S. E., Chronic wounds and the medical biofilm paradigm. *J Wound Care* **2010,** *19* (2), 45-6, 48-50, 52-3.

[25] Gallow, J.; Holinka, M.; Moucha, C. S., Antibacterial Surface Treatment for Orthopedic Implants. *International Journal of Molecular Sciences* **2014,** *15*, 13849-13880.

[26] Zhao, L.; Chu, P. K.; Zhang, Y.; Wu, Z., Antibacterial coatings on titanium implants. *J Biomed Mater Res B Appl Biomater* **2009,** *91* (1), 470-80.

[27] Silver, S.; Phung le, T.; Silver, G., Silver as biocides in burn and wound dressings and bacterial resistance to silver compounds. *J Ind Microbiol Biotechnol* **2006,** *33* (7), 627-34.

[28] Maillard, J. Y.; Hartemann, P., Silver as an antimicrobial: facts and gaps in knowledge. *Crit Rev Microbiol* **2013,** *39* (4), 373-83.

[29] Alexander, J. W., History of the medical use of silver. *Surg Infect (Larchmt)* **2009,** *10* (3), 289-92.

[30] Jelenko, C. *Silver nitrate resistant E. coli: report of case*; 1969; pp 296-299.

[31] Haefeli, C.; Franklin, C.; Hardy, K., Plasmid-determined silver resistance in Pseudomonas stutzeri isolated from a silver mine. *Journal of Bacteriology* **1984,** *158*, 389-392.

[32] Mijnendonckx, K.; Leys, N.; Mahillon, J.; Silver, S.; Van Houdt, R., Antimicrobial silver: uses, toxicity and potential for resistance. *Biometals* **2013,** *26* (4), 609-21.

[33] Edwards-Jones, V., The benefits of silver in hygiene, personal care and healthcare. *Lett Appl Microbiol* **2009,** *49* (2), 147-52.

[34] Percival, S. L.; Slone, W.; Linton, S.; Okel, T.; Corum, L.; Thomas, J. G., The antimicrobial efficacy of a silver alginate dressing against a broad spectrum of clinically relevant wound isolates. *Int Wound J* **2011,** *8* (3), 237-43.

[35] Chernousova, S.; Epple, M., Silver as antibacterial agent: ion, nanoparticle, and metal. *Angew Chem Int Ed Engl* **2013,** *52* (6), 1636-53.

[36] Lansdown, A. B., Critical observations on the neurotoxicity of silver. *Crit Rev Toxicol* **2007,** *37* (3), 237-50.

[37] Wan, A. T.; Conyers, R. A.; Coombs, C. J.; Masterton, J. P., Determination of silver in blood, urine, and tissues of volunteers and burn patients. *Clin Chem* **1991,** *37* (10 Pt 1), 1683-7.

[38] Bleehen, S. S.; Gould, D. J.; Harrington, C. I.; Durrant, T. E.; Slater, D. N.; Underwood, J. C., Occupational argyria; light and electron microscopic studies and X-ray microanalysis. *Br J Dermatol* **1981,** *104* (1), 19-26.

[39] Chung, I. S.; Lee, M. Y.; Shin, D. H.; Jung, H. R., Three systemic argyria cases after ingestion of colloidal silver solution. *Int J Dermatol* **2010,** *49* (10), 1175-7.

[40] Glehr, M.; Leithner, A.; Friesenbichler, J.; Goessler, W.; Avian, A.; Andreou, D.; Maurer-Ertl, W.; Windhager, R.; Tunn, P. U., Argyria following the use of silver-coated megaprostheses: no association between the development of local argyria and elevated silver levels. *Bone Joint J* **2013,** *95-B* (7), 988-92.

[41] Lansdown, A. B.; Williams, A., How safe is silver in wound care? *J Wound Care* **2004,** *13* (4), 131-6.

[42] Zheng, W.; Aschner, M.; Ghersi-Egea, J. F., Brain barrier systems: a new frontier in metal neurotoxicological research. *Toxicol Appl Pharmacol* **2003,** *192* (1), 1-11.

[43] Zheng, W., Toxicology of choroid plexus: special reference to metal-induced neurotoxicities. *Microsc Res Tech* **2001,** *52* (1), 89-103.

[44] Goebel, H. H.; Muller, J., Ultrastructural observations on silver deposition in the choroid plexus of a patient with argyria. *Acta Neuropathol* **1973,** *26* (3), 247-51.

[45] Klemm, P.; Vejborg, R. M.; Hancock, V., Prevention of bacterial adhesion. *Appl Microbiol Biotechnol* **2010,** *88* (2), 451-9.

[46] Fordham, W. R.; Redmond, S.; Westerland, A.; Cortes, E. G.; Walker, C.; Gallagher, C.; Medina, C. J.; Waecther, F.; Lunk, C.; Ostrum, R. F.; Caputo, G. A.; Hettinger, J. D.; Krchnavek, R. R., Silver as a Bactericidal Coating for Biomedical Implants. *Surface & Coatings Technology* **2014,** *253*, 52-57.

[47] Pritchard, E. M.; Szybala, C.; Boison, D.; Kaplan, D. L., Silk fibroin encapsulated powder reservoirs for sustained release of adenosine. *J Control Release* **2010,** *144* (2), 159-67.

[48] Cameron, D. *Antimicrobial Resistance: Tackling a crisis for the health and wealth of nations*; 2014.

[49] Suresh, A. K.; Doktycz, M. J.; Wang, W.; Moon, J. W.; Gu, B.; Meyer, H. M., 3rd; Hensley, D. K.; Allison, D. P.; Phelps, T. J.; Pelletier, D. A., Monodispersed biocompatible silver sulfide nanoparticles: facile extracellular biosynthesis using the gamma-proteobacterium, Shewanella oneidensis. *Acta Biomater* **2011,** *7* (12), 4253-8.

[50] Jain, J.; Arora, S.; Rajwade, J. M.; Omray, P.; Khandelwal, S.; Paknikar, K. M., Silver nanoparticles in therapeutics: development of an antimicrobial gel formulation for topical use. *Mol Pharm* **2009,** *6* (5), 1388-401.

[51] Panacek, A.; Kolar, M.; Vecerova, R.; Prucek, R.; Soukupova, J.; Krystof, V.; Hamal, P.; Zboril, R.; Kvitek, L., Antifungal activity of silver nanoparticles against Candida spp. *Biomaterials* **2009,** *30* (31), 6333-40.

[52] Hwang, M. G.; Katayama, H.; Ohgaki, S., Inactivation of Legionella pneumophila and Pseudomonas aeruginosa: evaluation of the bactericidal ability of silver cations. *Water Res* **2007,** *41* (18), 4097-104.

[53] Russell, A. D.; Hugo, W. B., Antimicrobial activity and action of silver. *Prog Med Chem* **1994,** *31*, 351-70.

[54] Chole, R. A.; Hubbell, R. N., Antimicrobial activity of silastic tympanostomy tubes impregnated with silver oxide. A double-blind randomized multicenter trial. *Arch Otolaryngol Head Neck Surg* **1995,** *121* (5), 562-5.

[55] Schaeffer, A. J.; Story, K. O.; Johnson, S. M., Effect of silver oxide/trichloroisocyanuric acid antimicrobial urinary drainage system on catheter-associated bacteriuria. *J Urol* **1988,** *139* (1), 69-73.

[56] Tripathi, S.; Mehrotra, G. K.; Dutta, P. K., Chitosan–silver oxide nanocomposite film: Preparation and antimicrobial activity. *Bulletin of Materials Science* **2011,** *34* (1), 29-35.

[57] Hettinger, J., Silver oxide coatings with high silver-ion elution rates for bactericidal applications. *unpublished*.

[58] Anderl, J. N.; Franklin, M. J.; Stewart, P. S., Role of antibiotic penetration limitation in Klebsiella pneumoniae biofilm resistance to ampicillin and ciprofloxacin. *Antimicrob Agents Chemother* **2000,** *44* (7), 1818-24.

[59] Demidova, T. N.; Hamblin, M. R., Effect of cell-photosensitizer binding and cell density on microbial photoinactivation. *Antimicrob Agents Chemother* **2005,** *49* (6), 2329-35.

[60] Wang, H. H.; Isaacs, F. J.; Carr, P. A.; Sun, Z. Z.; Xu, G.; Forest, C. R.; Church, G. M., Programming cells by multiplex genome engineering and accelerated evolution. *Nature* **2009,** *460* (7257), 894-8.

[61] Sambale, F.; Wagner, S.; Stahl, F.; Khaydarov, R. R.; Scheper, T.; Bahnemann, D., Investigations of the Toxic Effect of Silver Nanoparticles on Mammalian Cell Lines. *Journal of Nanomaterials* **2015,** *2015*, 1-9.

[62] Bockstael, K.; Aerschot, A. V., Antimicrobial Resistance in Bacteria. *Central European Journal of Medicine* **2008,** *4* (2), 141-155.

[63] Duran, N.; Duran, M.; de Jesus, M. B.; Seabra, A. B.; Favaro, W. J.; Nakazato, G., Silver nanoparticles: A new view on mechanistic aspects on antimicrobial activity. *Nanomedicine* **2016,** *12* (3), 789-99.

[64] Lara, H. H. L.; Ayala-Núñez, N. V.; del Carmen Ixtepan Turrent, L.; Rodríguez Padilla, C., Bactericidal effect of silver nanoparticles against multidrug-resistant bacteria. *World Journal of Microbiology and Biotechnology* **2010,** *26* (4), 615-621.

[65] Markowska, K.; Grudniak, A. M.; Wolska, K. I., Silver nanoparticles as an alternative strategy against bacterial biofilms. *Acta Biochim Pol* **2013,** *60* (4), 523-30.

[66] Singh, R.; Shedbalkar, U. U.; Wadhwani, S. A.; Chopade, B. A., Bacteriagenic silver nanoparticles: synthesis, mechanism, and applications. *Appl Microbiol Biotechnol* **2015,** *99* (11), 4579-93.

[67] Chopra, I., The increasing use of silver-based products as antimicrobial agents: a useful development or a cause for concern? *J Antimicrob Chemother* **2007,** *59* (4), 587-90.

[68] van de Belt, H.; Neut, D.; Schenk, W.; van Horn, J. R.; van Der Mei, H. C.; Busscher, H. J., Staphylococcus aureus biofilm formation on different gentamicin-loaded polymethylmethacrylate bone cements. *Biomaterials* **2001,** *22* (12), 1607-11.

[69] Hendriks, J. G.; Neut, D.; van Horn, J. R.; van der Mei, H. C.; Busscher, H. J., Bacterial survival in the interfacial gap in gentamicin-loaded acrylic bone cements. *J Bone Joint Surg Br* **2005,** *87* (2), 272-6.

[70] Miola, M.; Fucale, G.; Maina, G.; Verne, E., Antibacterial and bioactive composite bone cements containing surface silver-doped glass particles. *Biomed Mater* **2015,** *10* (5), 055014.

[71] Hebeish, A.; El-Rafie, M. H.; El-Sheikh, M. A.; Seleem, A. A.; El-Naggar, M. E., Antimicrobial wound dressing and anti-inflammatory efficacy of silver nanoparticles. *Int J Biol Macromol* **2014,** *65*, 509-15.

[72] Rai, M.; Yadav, A.; Gade, A., Silver nanoparticles as a new generation of antimicrobials. *Biotechnol Adv* **2009,** *27* (1), 76-83.

[73] Amin, Y. M.; Hawas, A. M.; El-Batal, A. I.; Hassan, S. H. M.; Elsayed, M. E., Evaluation of Acute and Subchronic Toxicity of Silver Nanoparticles in Normal and Irradiated Animals. *British Journal of Pharmacology and Toxicology* **2015,** *6* (2), 22-38.

[74] Maneewattanapinyo, P.; Banlunara, W.; Thammacharoen, C.; Ekgasit, S.; Kaewamatawong, T., An evaluation of acute toxicity of colloidal silver nanoparticles. *J Vet Med Sci* **2011,** *73* (11), 1417-23.

[75] Retchkiman-Schabes, P. S.; Canizal, G.; Becerra-Herrera, R.; Zorrilla, C.; Liu, H.B.; Ascencio, J. A., Biosynthesis and characterization of Ti/Ni bimetallic nanoparticles. *Optical Materials* **2006,** *29*, 95-99.

[76] Gu, H.; Ho, P. L.; Tong, E.; Wang, L.; Hu, B., Presenting vancomycin on nanoparticles to enhance antimicrobial activities. *Nano Letters* **2003,** *3* (9), 1261-1263.

[77] Ahmad, Z.; Pandey, R.; Sharma, S.; Khuller, G. K., Alginate nanoparticles as antituberculosis drug carriers: formulation development, pharmacokinetics and therapeutic potential. *Indian J Chest Dis Allied Sci* **2006,** *48* (3), 171-6.

[78] Suresh, A. K.; Pelletier, D. A.; Wang, W.; Moon, J. W.; Gu, B.; Mortensen, N. P.; Allison, D. P.; Joy, D. C.; Phelps, T. J.; Doktycz, M. J., Silver nanocrystallites: biofabrication using Shewanella oneidensis, and an evaluation of their comparative toxicity on gram-negative and gram-positive bacteria. *Environ Sci Technol* **2010,** *44* (13), 5210-5.

[79] Hadrup, N.; Lam, H. R., Oral toxicity of silver ions, silver nanoparticles and colloidal silver--a review. *Regul Toxicol Pharmacol* **2014,** *68* (1), 1-7.

[80] Kim, Y. S.; Kim, J. S.; Cho, H. S.; Rha, D. S.; Kim, J. M.; Park, J. D.; Choi, B. S.; Lim, R.; Chang, H. K.; Chung, Y. H.; Kwon, I. H.; Jeong, J.; Han, B. S.; Yu, I. J., Twenty-eight-day oral toxicity, genotoxicity, and gender-related tissue distribution of silver nanoparticles in Sprague-Dawley rats. *Inhal Toxicol* **2008,** *20* (6), 575-83.

[81] Damm, C.; Münstedt, H., Kinetic aspects of the silver ion release from antimicrobial polyamide/silver nanocomposites. *Applied Physics A* **2008,** *91* (3), 479-486.

[82] Saidi, I. S.; Biedlingmaier, J. F.; Whelan, P., In vivo resistance to bacterial biofilm formation on tympanostomy tubes as a function of tube material. *Otolaryngol Head Neck Surg* **1999,** *120* (5), 621-7.

[83] Agarwal, A.; Weis, T. L.; Schurr, M. J.; Faith, N. G.; Czuprynski, C. J.; McAnulty, J. F.; Murphy, C. J.; Abbott, N. L., Surfaces modified with nanometer-thick silver-impregnated polymeric films that kill bacteria but support growth of mammalian cells. *Biomaterials* **2010,** *31* (4), 680-90.

[84] Roy, M.; Fielding, G. A.; Beyenal, H.; Bandyopadhyay, A.; Bose, S., Mechanical, in vitro antimicrobial, and biological properties of plasma-sprayed silver-doped hydroxyapatite coating. *ACS Appl Mater Interfaces* **2012,** *4* (3), 1341-9.

[85] Li, B.; Liu, X.; Cao, C.; Dong, Y.; Ding, C., Biological and antibacterial properties of plasma sprayed wollastonite/silver coatings. *J Biomed Mater Res B Appl Biomater* **2009,** *91* (2), 596-603.

[86] Chen, W.; Liu, Y.; Courtney, H. S.; Bettenga, M.; Agrawal, C. M.; Bumgardner, J.D.; Ong, J. L., In vitro anti-bacterial and biological properties of magnetron co-sputtered silver-containing hydroxyapatite coating. *Biomaterials* **2006,** *27* (32), 5512-7.

[87] Eto, S.; Miyamoto, H.; Shobuike, T.; Noda, I.; Akiyama, T.; Tsukamoto, M.; Ueno, M.; Someya, S.; Kawano, S.; Sonohata, M.; Mawatari, M., Silver oxide-containing hydroxyapatite coating supports osteoblast function and enhances implant anchorage strength in rat femur. *J Orthop Res* **2015,** *33* (9), 1391-7.

[88] Gholipourmalekabadi, M.; Nezafati, N.; Hajibaki, L.; Mozafari, M.; Moztarzadeh, F.; Hesaraki, S.; Samadikuchaksaraei, A., Detection and qualification of optimum antibacterial and cytotoxic activities of silver-doped bioactive glasses. *IET Nanobiotechnol* **2015,** *9* (4), 209-14.

[89] Ostrum, R.; Hettinger, J.; Krchnavek, R.; Caputo, G. A. Use of Silver-Containing Layers at Implant Surfaces. 2013.

[90] Zhao, G.; Stevens, S. E., Jr., Multiple parameters for the comprehensive evaluation of the susceptibility of Escherichia coli to the silver ion. *Biometals* **1998,** *11* (1), 27-32.

[91] Bovenkamp, G. L.; Zanzen, U.; Krishna, K. S.; Hormes, J.; Prange, A., X-ray absorption near-edge structure (XANES) spectroscopy study of the interaction of silver ions with Staphylococcus aureus, Listeria monocytogenes, and Escherichia coli. *Appl Environ Microbiol* **2013,** *79* (20), 6385-90.

[92] Tien, D. C.; Tseng, K. H.; Liao, C. Y.; Tsung, T. T., Colloidal silver fabrication using the spark discharge system and its antimicrobial effect on Staphylococcus aureus. *Med Eng Phys* **2008,** *30* (8), 948-52.

[93] Low, W. L.; Martin, C.; Hill, D. J.; Kenward, M. A., Antimicrobial efficacy of silver ions in combination with tea tree oil against Pseudomonas aeruginosa, Staphylococcus aureus and Candida albicans. *Int J Antimicrob Agents* **2011,** *37* (2), 162-5.

[94] Feng, Q. L.; Wu, J.; Chen, G. Q.; Cui, F. Z.; Kim, T. N.; Kim, J. O., A mechanistic study of the antibacterial effect of silver ions on Escherichia coli and Staphylococcus aureus. *J Biomed Mater Res* **2000,** *52* (4), 662-8.

[95] Kawahara, K.; Tsuruda, K.; Morishita, M.; Uchida, M., Antibacterial effect of silver-zeolite on oral bacteria under anaerobic conditions. *Dental Materials* **2000,** *16* (6), 452-455.

[96] Babu, R.; Zhang, J.; Beckman, E. J.; Virji, M.; Pasculle, W. A.; Wells, A., Antimicrobial activities of silver used as a polymerization catalyst for a wound-healing matrix. *Biomaterials* **2006,** *27* (24), 4304-14.

[97] Panacek, A.; Smekalova, M.; Vecerova, R.; Bogdanova, K.; Roderova, M.; Kolar, M.; Kilianova, M.; Hradilova, S.; Froning, J. P.; Havrdova, M.; Prucek, R.; Zboril, R.; Kvitek, L., Silver nanoparticles strongly enhance and restore bactericidal activity of inactive antibiotics against multiresistant Enterobacteriaceae. *Colloids Surf B Biointerfaces* **2016,** *142*, 392-9.

[98] Brett, D. W., A discussion of silver as an antimicrobial agent: alleviating the confusion. *Ostomy Wound Manage* **2006,** *52* (1), 34-41.

[99] Sant, S. B.; Gill, K. S.; Burrell, R. E., Nanostructure, dissolution and morphology characteristics of microcidal silver films deposited by magnetron sputtering. *Acta Biomater* **2007,** *3* (3), 341-50.

[100] Dale, H.; Hallan, G.; Hallan, G.; Espehaug, B.; Havelin, L. I.; Engesaeter, L. B., Increasing risk of revision due to deep infection after hip arthroplasty. *Acta Orthop* **2009,** *80* (6), 639-45.

[101] Billings, N.; Birjiniuk, A.; Samad, T. S.; Doyle, P. S.; Ribbeck, K., Material properties of biofilms-a review of methods for understanding permeability and mechanics. *Rep Prog Phys* **2015,** *78* (3), 036601.

[102] Bjarnsholt, T.; Alhede, M.; Eickhardt-Sørensen, S. R.; Moser, C.; Kühl, M.; Jensen, P. O.; Høiby, N., The in vivo biofilm. *Trends in Microbiology* **2013,** *September 2013* (21), 466-474.

[103] Romling, U.; Kjelleberg, S.; Normark, S.; Nyman, L.; Uhlin, B. E.; Akerlund, B., Microbial biofilm formation: a need to act. *J Intern Med* **2014,** *276* (2), 98-110.

[104] Lebeaux, D.; Chauhan, A.; Rendueles, O.; Beloin, C., From in vitro to in vivo models of bacterial biofilm-related infections. *Pathogens* **2013,** *2* (2), 288-356.

[105] Silver, S., Bacterial silver resistance: molecular biology and uses and misuses of silver compounds. *FEMS Microbiol Rev* **2003,** *27* (2-3), 341-53.

[106] Randall, C. P.; Gupta, A.; Jackson, N.; Busse, D.; O'Neill, A. J., Silver resistance in Gram-negative bacteria: a dissection of endogenous and exogenous mechanisms. *J Antimicrob Chemother* **2015,** *70* (4), 1037-46.

[107] Olfert, E. D.; Godson, D. L., Humane Endpoints for Infectious Disease Animal Models. *ILAR Journal* **2000,** *41* (2), 99-104.

[108] Kaba, S. I.; Egorova, E. M., In vitro studies of the toxic effects of silver nanoparticles on HeLa and U937 cells. *Nanotechnol Sci Appl* **2015,** *8*, 19-29.

[109] Coenye, T.; Nelis, H. J., In vitro and in vivo model systems to study microbial biofilm formation. *J Microbiol Methods* **2010,** *83* (2), 89-105.

[110] Olcott, C. T., Experimental Argyrosis: III. Pigmentation of the Eyes of Rats Following Ingestion of Silver During Long Periods of Time. *Am J Pathol* **1947,** *23* (5), 783-91.

[111] Olcott, C. T., Experimental argyrosis; morphologic changes in the experimental animal. *Am J Pathol* **1948,** *24* (4), 813-33.

[112] Olcott, C. T., Experimental argyrosis; hypertrophy of the left ventricle of the heart in rats ingesting silver salts. *AMA Arch Pathol* **1950,** *49* (2), 138-49.

[113] Olcott, C. T.; Richter, G. W., Experimental argyrosis. VI. Electron microscopic study of ingested silver in the kidney of the rat. *Lab Invest* **1958,** *7* (2), 103-9.

[114] Loeschner, K.; Hadrup, N.; Qvortrup, K.; Larsen, A.; Gao, X.; Vogel, U.; Mortensen, A.; Lam, H. R.; Larsen, E. H., Distribution of silver in rats following 28 days of repeated oral exposure to silver nanoparticles or silver acetate. *Part Fibre Toxicol* **2011,** *8*, 18.

[115] Rungby, J., Experimental argyrosis: ultrastructural localization of silver in rat eye. *Exp Mol Pathol* **1986,** *45* (1), 22-30.

[116] Rungby, J.; Danscher, G., Localization of exogenous silver in brain and spinal cord of silver exposed rats. *Acta Neuropathol* **1983,** *60* (1-2), 92-8.

[117] Pereira, G., Localization of silver in the spleen of argyric rats by energy dispersive X-ray analysis coupled with scanning and transmission electron microscopy. *Proc. Annu Meet. Electron Microscopy Soc. Am.* **1977,** *35*, 504-505.

[118] van der Zande, M.; Vandebriel, R. J.; Van Doren, E.; Kramer, E.; Herrera Rivera, Z.; Serrano-Rojero, C. S.; Gremmer, E. R.; Mast, J.; Peters, R. J.; Hollman, P. C.; Hendriksen, P. J.; Marvin, H. J.; Peijnenburg, A. A.; Bouwmeester, H., Distribution, elimination, and toxicity of silver nanoparticles and silver ions in rats after 28-day oral exposure. *ACS Nano* **2012,** *6* (8), 7427-42.

[119] Walker, F., The deposition of silver in glomerular basement membrane. *Virchows Arch B Cell Pathol* **1972,** *11* (1), 90-6.

[120] Walker, F., Experimental argyria: a model for basement membrane studies. *Br J Exp Pathol* **1971,** *52* (6), 589-93.

[121] Eaglstein, W. H.; Sullivan, T. P.; Giordano, P. A.; Miskin, B. M., A liquid adhesive bandage for the treatment of minor cuts and abrasions. *Dermatol Surg* **2002,** *28* (3), 263-7.

[122] Colvin, K. M.; Gordon, V. D.; Murakami, K.; Borlee, B. R.; Wozniak, D. J.; Wong, G. C.; Parsek, M. R., The pel polysaccharide can serve a structural and protective role in the biofilm matrix of Pseudomonas aeruginosa. *PLoS Pathog* **2011,** *7* (1), e1001264.

[123] Shelke, N. B.; James, R.; Loaurencin, C. T.; Kumbar, S. G., Polysaccharide biomaterials for drug delivery and regenerative engineering. *Polymers for Advanced Technologies* **2014,** (25), 448-460.

[124] Hu, X.; Wang, X.; Rnjak, J.; Weiss, A. S.; Kaplan, D. L., Biomaterials derived from silk-tropoelastin protein systems. *Biomaterials* **2010,** *31* (32), 8121-31.

[125] Jin, H. J.; Kaplan, D. L., Mechanism of silk processing in insects and spiders. *Nature* **2003,** *424* (6952), 1057-61.

[126] Hu, X.; Lu, Q.; Kaplan, D. L.; Cebe, P., Microphase separation controlled beta-sheet crystallization kinetics in fibrous proteins. *Macromolecules* **2009,** (42), 2079-2087.

[127] Hu, X.; Kaplan, D.; Cebe, P., Dynamic protein-water relationships during beta-sheet formation. *Macromolecules* **2008,** (41), 3939-3948.

[128] Hu, X.; Kaplan, D.; Cebe, P., Effect of water on the thermal properties of silk fibroin. *Thermochim Acta* **2007,** (461), 137-144.

[129] Hu, X.; Kaplan, D.; Cebe, P., Determining beta-sheet crystallinity in fibrous proteins by thermal analysis and infared spectroscopy. *Macromolecules* **2006,** (39), 6161-6170.

[130] Shang, S.; Zhu, L.; Fan, J., Intermolecular interactions between natural polysaccharides and silk fibroin protein. *Carbohydr Polym* **2013,** *93* (2), 561-73.

[131] Davis, S. C.; Cazzaniga, A. L.; Eaglstein, W. H.; Mertz, P. M., Over-the-counter topical antimicrobials: effective treatments? *Arch Dermatol Res* **2005,** *297* (5), 190-5.

[132] Leyden, J. J.; Bartelt, N. M., Comparison of topical antibiotic ointments, a wound protectant, and antiseptics for the treatment of human blister wounds contaminated with Staphylococcus aureus. *J Fam Pract* **1987,** *24* (6), 601-4.

[133] Boonkaew, B.; Kempf, M.; Kimble, R.; Supaphol, P.; Cuttle, L., Antimicrobial efficacy of a novel silver hydrogel dressing compared to two common silver burn wound dressings: Acticoat and PolyMem Silver((R)). *Burns* **2014,** *40* (1), 89-96.

[134] Abedini, F.; Ahmadi, A.; Yavari, A.; Hosseini, V.; Mousavi, S., Comparison of silver nylon wound dressing and silver sulfadiazine in partial burn wound therapy. *Int Wound J* **2013,** *10* (5), 573-8.

[135] Prestes, M. A.; Ribas, C. A.; Ribas Filho, J. M.; Moreira, L. B.; Boldt, A. B.; Brustolin, E. V.; Castanho, L. S.; Bernardi, J. A.; Dias, F. C., Wound healing using ionic silver dressing and nanocrystalline silver dressing in rats. *Acta Cir Bras* **2012,** *27* (11), 761-7.

[136] Lo, S. F.; Chang, C. J.; Hu, W. Y.; Hayter, M.; Chang, Y. T., The effectiveness of silver-releasing dressings in the management of non-healing chronic wounds: a meta-analysis. *J Clin Nurs* **2009,** *18* (5), 716-28.

[137] Hobman, J. L.; Crossman, L. C., Bacterial antimicrobial metal ion resistance. *J Med Microbiol* **2015,** *64* (Pt 5), 471-97.

[138] Grass, G.; Rensing, C.; Solioz, M., Metallic Copper as an Antimicrobial. *Applied and Enviornmental Microbiology* **2011,** (77), 1541-1547.

[139] Kapel, D. The Antimicrobial Metal. http://www.thefreelibrary.com/The+antimicrobial+metal%3a+copper+alloy+registration+offers...-a0307185492 (accessed June 1).

[140] Moseke, C.; Gbureck, U.; Elter, P.; Drechsler, P.; Zoll, A.; Thull, R.; Ewald, A., Hard implant coatings with antimicrobial properties. *J Mater Sci Mater Med* **2011,** *22* (12), 2711-20.

[141] Kumar, R.; Munstedt, H., Silver ion release from antimicrobial polyamide/silver composites. *Biomaterials* **2005,** *26* (14), 2081-8.

[142] Haynes, W. M., *CRC Handbook of Chemistry and Physics: A ready-reference book of chemical and physical data*. CRC Press: Boca Raton, 2009.

[143] Murphy, A. R.; St John, P.; Kaplan, D. L., Modification of silk fibroin using diazonium coupling chemistry and the effects on hMSC proliferation and differentiation. *Biomaterials* **2008,** *29* (19), 2829-38.

[144] Ha, S. W.; Gracz, H. S.; Tonelli, A. E.; Hudson, S. M., Structural study of irregular amino acid sequences in the heavy chain of Bombyx mori silk fibroin. *Biomacromolecules* **2005,** *6* (5), 2563-9.